

## PROJECT ADMINISTRATION DATA SHEET

☒ ORIGINAL ☐ REVISION NO. \_\_\_\_\_Project No. G-33-681GTRI/GIT DATE 3 / 9 / 84Project Director: Dr. E.M. BurgessSchool/~~Lab~~ ChemistrySponsor: National Institute of General Medical Sciences/DHHS/PHS  
Bethesda, MDType Agreement: Grant No. 5 R01 GM31930-02Award Period: From 4/1/84 To 3/31/85 (Performance) 6/30/85 (Reports)Sponsor Amount: This Change Total to DateEstimated: \$ \_\_\_\_\_ \$ 100,666Funded: \$ \_\_\_\_\_ \$ 100,666Cost Sharing Amount: \$ 5,298 Cost Sharing No: G-33-385Title: Acyclic Stereoselection

## ADMINISTRATIVE DATA

OCA Contact John W. Burdette x4820

## 1) Sponsor Technical Contact:

## 2) Sponsor Admin/Contractual Matters:

Dr. Carl A. KuetherAnn Calure/Jeff CarowProgram AdministratorGrants Management SpecialistNational Institute of General MedicalOffice of Associate Director forSciencesProgram ActivitiesBethesda, MD 20205Nat'l Institute of Gen'l Medical Sciences(301) 496-7181Bethesda, MD 20205 (301)496-7166Defense Priority Rating: n/aMilitary Security Classification: n/a(or) Company/Industrial Proprietary: n/a

## RESTRICTIONS

See Attached NIH Supplemental Information Sheet for Additional Requirements.

Travel: Foreign travel must have prior approval - Contact OCA in each case. Domestic travel requires sponsor approval where total will exceed greater of \$500 or 125% of approved proposal budget category.

Equipment: Title vests with GIT

## COMMENTS:



## COPIES TO:

I.D. No. 02.108.001.84.012

Project Director  
Research Administrative Network  
Research Property Management  
AccountingProcurement/EES Supply Services  
Research Security Services  
Reports Coordinator (OCA)  
Research Communications (2)GTRI  
Library  
Project File  
Other NEWTON

## SPONSORED PROJECT TERMINATION/CLOSEOUT SHEET

Date January 29, 1986Project No. G-33-681School/~~XXX~~ ChemistryIncludes Subproject No.(s) N/AProject Director(s) Dr. E.M. BurgessGTRC /~~XXX~~Sponsor National Institute of General Medical Sciences/DHHS/PHSTitle Acyclic StereoselectionEffective Completion Date: 3/31/85 (Performance) 6/30/85 (Reports)

## Grant/Contract Closeout Actions Remaining:

- ☐ None
- ☒ ~~Final Fiscal Report~~ Final Fiscal Report
- ☐ Closing Documents
- ☒ Final Report of Inventions 568 sent to Project Director
- ☐ Govt. Property Inventory & Related Certificate
- ☐ Classified Material Certificate
- ☐ Other \_\_\_\_\_

Continues Project No. \_\_\_\_\_

Continued by Project No. G-33-641

## COPIES TO:

Project Director  
Research Administrative Network  
Research Property Management  
Accounting  
Procurement/GTRI Supply Services  
Research Security Services  
Reports Coordinator (OCA)  
Legal Services

Library  
GTRC  
Research Communications (2)  
Project File  
Other Heyser, Jones, Embry

C. Progress Report

(1) The beginning and ending dates for the period covered since the project was last reviewed competitively are 4/1/83 and 3/31/86, respectively.

(2) Professional Personal Working on Project:

<u>Name</u>	<u>Title</u>	<u>Dates of Service</u>	<u>Percentage Time</u>
Burgess, E. M.	Professor	7/1/83 - present	12
Liotta, C. L.	Professor	7/1/83 - present	12
McCraw, E.	Grad. Stud.	6/20/83-9/3/83	45
Mitchell, K.	Grad. Stud.	6/20/83-9/3/83	45
Pham, V.	Grad. Stud.	3/26/84-3/23/85	45
White, S.	Grad. Stud.	6/20/83-9/3/83	45
Duff, J.	Grad. Stud.	3/26/84-3/23/85	45
Le Roux, S.	Grad. Stud.	6/20/83-3/23/85	45
Earnhardt, L.	Grad. Stud.	6/18/84-12/8/84	45
		6/20/83-12/10/83	45
		9/19/83-12/10/83	45

(3) The Specific Aims of the previous application were

(a) to develop a qualitative theoretical model to describe the attractive electronic (stabilizing) terms in the attack of a nucleophile at a  $\pi$ -electrophilic center,

(b) to use the model in predicting the magnitude of asymmetric induction accompanying nucleophilic attack at an  $\alpha$ -chiral  $\pi$ -electrophilic center, and

(c) to initiate an experimental program to verify the model.

(4) Summary of Results

For convenience and clarity the "Summary of Results" is incorporated into the body of the section entitled "Experimental Design and Methods."



## D. Experimental Design and Methods

### Theoretical Results

In a series of papers (see appendix A, B, C, and D)<sup>1-4</sup>, a molecular orbital model describing the minimum energy trajectory of a nucleophile approaching a  $\pi$ -electrophilic center and the corresponding trajectory reaction windows is discussed in terms of the trajectory angles  $\theta$  and  $\phi$  (Figure 1).<sup>1-4</sup> The parameter  $\theta$

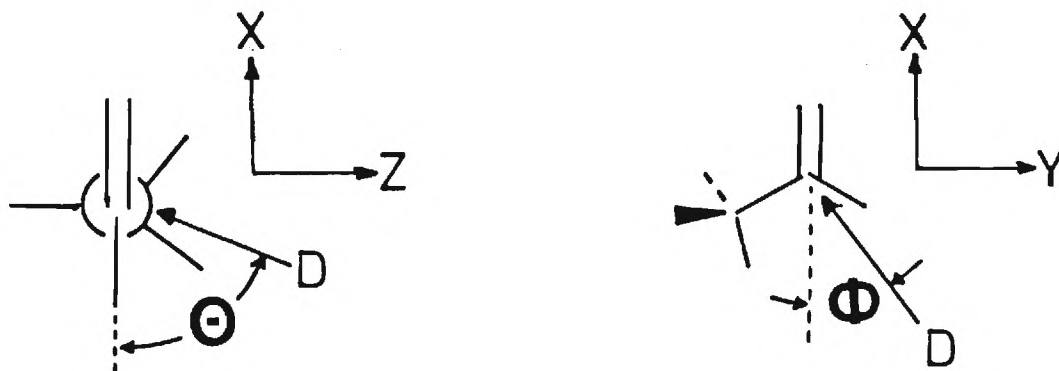


Figure 1

and  $\phi$  represent the approach angles of a nucleophilic donor, D, with respect to the  $\pi$ -plane and the  $\sigma$ -plane, respectively. The corresponding reaction windows,  $\omega(\theta)$  and  $\omega(\phi)$ , are defined as the change in  $\theta$  and  $\phi$  as a function of the change in the energy of interaction between the nucleophile and the  $\pi$ -electrophile. The model used to calculate these trajectory angles and windows involves analysis of:

- (1) short-ranged two-electron stabilizing (charge transfer) and four-electron destabilizing (repulsion) intermolecular forces resulting from overlap of the molecular orbitals of the reaction partners (orbital components), and
- (2) the longer-ranged electrostatic forces resulting from the interaction of the charge at the nucleophilic center with the electronic charge distribution at the  $\pi$ -electrophilic center (electrostatic component).



Clearly, the total energy of interaction between a given nucleophile and a given  $\pi$ -electrophile could be calculated at any point on the reaction surface by means of ab initio or semi-empirical molecular orbital techniques as well as by means of force-field methods. However, insight into the structural components of the nucleophile and the  $\pi$ -electrophile which effect the angular parameters  $\theta$ ,  $\phi$ ,  $\omega(\theta)$ , and  $\omega(\phi)$  would not be as evident. It is important to understand the origin of these parameters since they are directly related to the magnitude of asymmetric induction accompanying nucleophile attack at an  $\alpha$ -chiral  $\pi$ -electrophile center.

Consider, for example, a  $\pi$ -electrophile with an  $\alpha$ -chiral center. During the course of reaction with a nucleophile it would be anticipated that the magnitude of asymmetry induced at the prochiral  $\pi$ -center would be directly related to the angular parameters  $\theta$ ,  $\phi$ ,  $\omega(\theta)$  and  $\omega(\phi)$ . In particular, a small  $\theta$  value with a value of  $\phi$  in the quadrant containing the  $\alpha$ -chiral center accompanied by small  $\omega(\theta)$  and  $\omega(\phi)$  reaction windows would result in a high degree of asymmetric induction.

The trajectory model, based upon the dissection of the total energy into its orbital and electrostatic components, suggests several important structural generalizations for maximizing asymmetric induction. For a given  $\pi$ -electrophile,

- (a) as the energy of the highest occupied molecular orbital of the nucleophile ( $E_N$ ) becomes more negative, the charge transfer component of  $\theta$  approaches  $0^\circ$ ,
- (b) as the HOMO atomic orbital coefficient at the nucleophilic center ( $c_{pN}$ ) gets larger, the charge transfer and repulsion components of  $\omega(\phi)$  get smaller,
- (c) as the charge at the nucleophilic center ( $q_N$ ) gets smaller, the electrostatic component of  $\theta$  approaches  $0^\circ$ , and
- (d) as the distance between the nucleophile and the  $\pi$ -center increases the electrostatic component of  $\theta$  approaches  $0^\circ$ .

Thus, the magnitude of asymmetric induction should be great when the nucleophile has a low-lying HOMO with a large  $c_{pN}$  and a small value of  $q_N$  at the nucleophilic center.

The angular parameter  $\phi$  arises primarily from the structural characteristics of the  $\pi$ -electrophile. Some representative examples are shown in Figure 2. Based upon the examples, the following generalizations may be advanced:

- (1) The magnitude of asymmetric induction accompanying nucleophilic attack at an  $\alpha$ -chiral aldehyde should be greater under acid-catalyzed conditions (2 and 3) as compared to base-catalyzed conditions (1) since  $\theta$  has a smaller value and  $\phi$  is closer to the  $\alpha$ -chiral substituent in the former cases (2 and 3).
- (2) The magnitude of asymmetric induction accompanying a Michael addition to a  $\alpha$ -chiral activated alkene should be modestly great for the cis-isomer (5) as compared to the trans-counterpart (4) since the difference in  $\theta$  and  $\phi$  values are small.

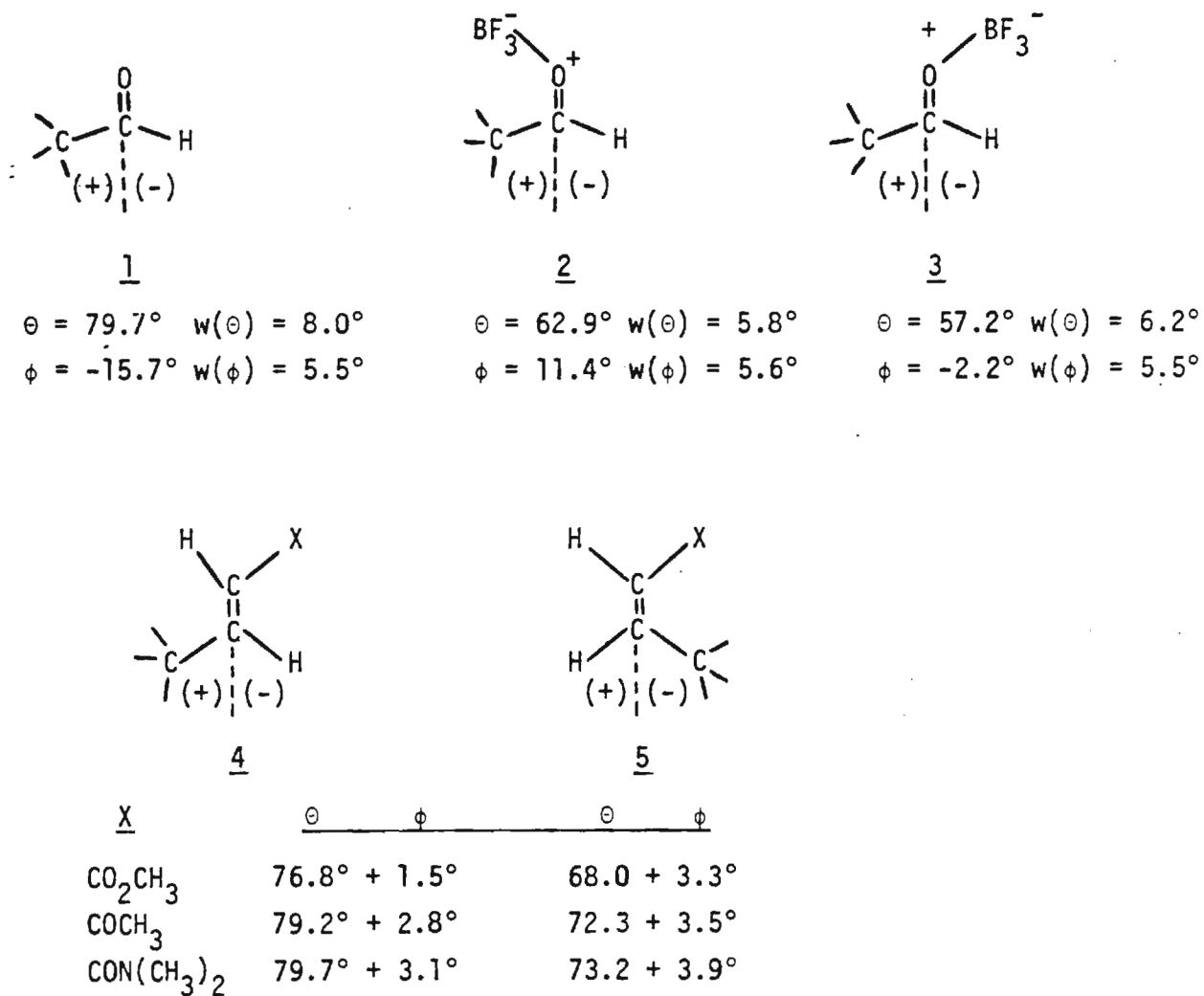


Figure 2

In contrast when the activating substituent is a thioester, a sulfoxide or a sulfone, (Figure 3), the trajectory model predicts that the cis - isomers (7,9,10) will produce substantially larger magnitude of asymmetric induction as compared to the trans-counterparts (6,8,10)

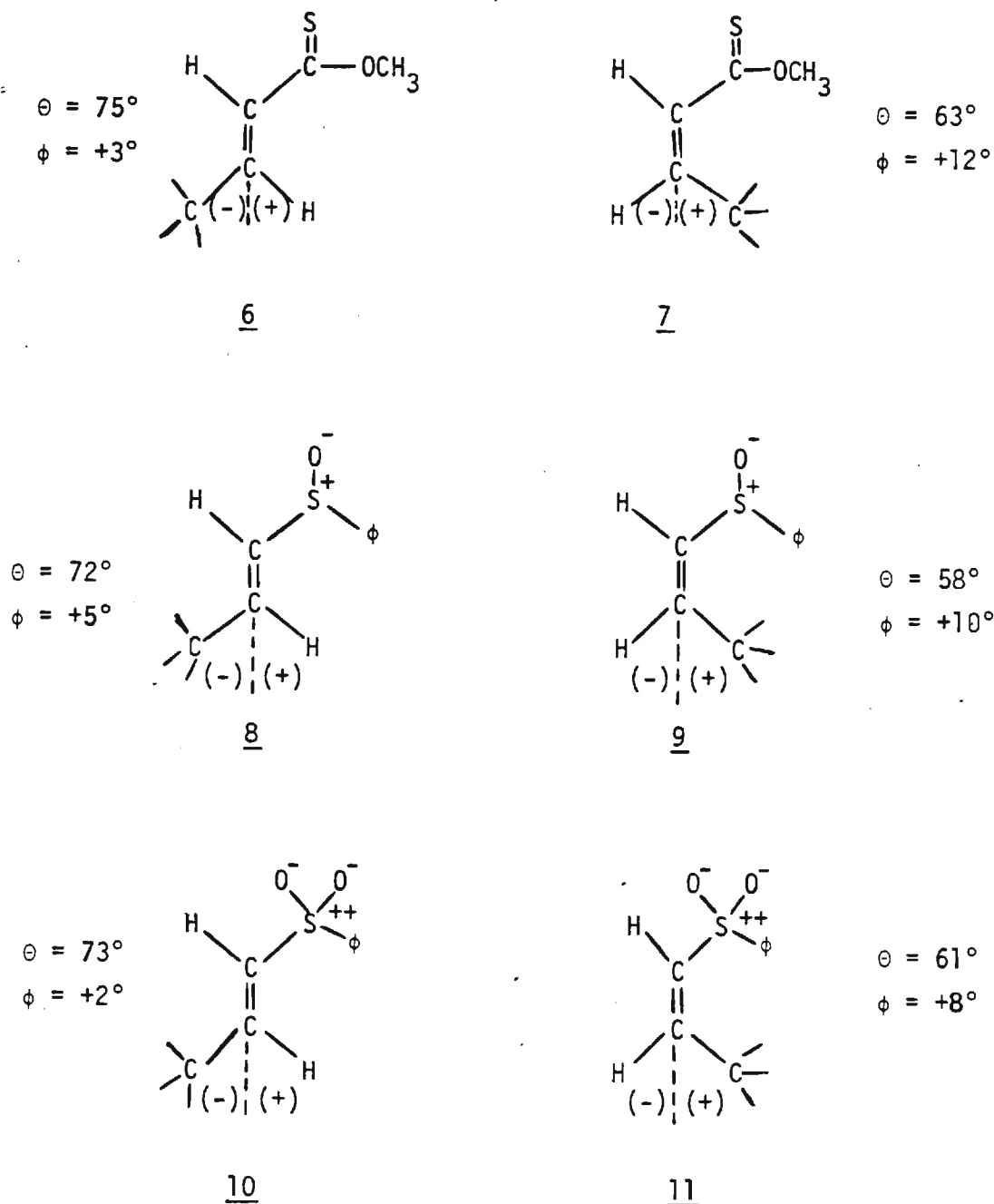


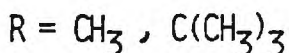
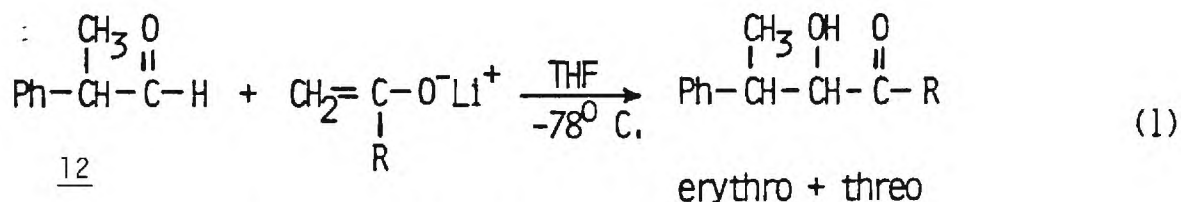
Figure 3



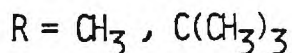
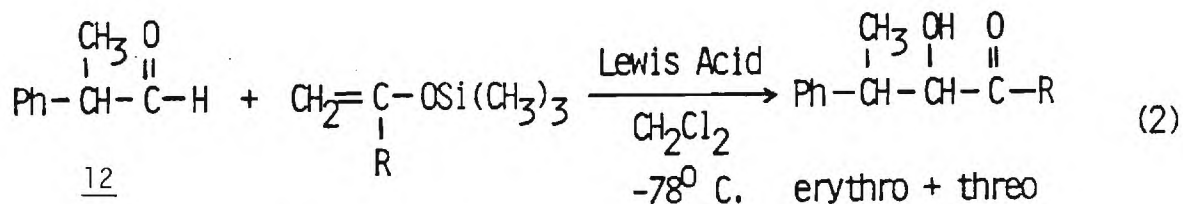
Experimental Results

The stereochemical course of the following aldol reaction systems have been investigated in our laboratories:

- (1) 2-phenylpropanol with the lithium enolates derived from acetone and pinacolone (Equation 1), and



- (2) 2-phenylpropanol with the silyl enol ethers derived from acetone and pinacolone in the presence of a variety of Lewis acids (Equation 2).



The results are summarized in Tables 1 and 2. The proposed trajectory model predicts that acid-catalyzed reactions with  $\alpha$ -chiral carbonyl  $\pi$ -electrophiles should proceed with greater diastereoselection as compared with the base-catalyzed counterpart. The results listed in Tables 1 and 2 and those of Heathcock and Flippin<sup>5</sup> are consistent with the predictions.

In addition to the relative diastereoselectivities, several interesting observations emerge from the data in Tables 1 and 2.

- (a) Under basic conditions the erythro-threo ratio and the absolute yield of aldol products appears to be independent of the presence of the lithium cation complexing agent, benzo-14-crown-4. Initially, it was conjectured that the 82:18 diastereomer ratio was the thermodynamic ratio and did not reflect the kinetics product distribution. However, several mixtures of diastereomers enriched in one or the other component were prepared and subjected to the conditions of the reaction. At room temperature equilibration did take place. A 75:25 ratio was observed. However, at  $-78^\circ\text{C}$  equilibration (in the absence or presence of benzo 14-crown 4) was negligibly slow implying that the ratios listed in Table 1 and 2 are kinetic product ratios. It was concluded that the benzo 14-crown-4 did

Table 2

Reagents		Diastereomeric Rates	Yield (%)
Nucleophile	Catalyst	erythro - threo	
$\begin{array}{c} \text{OLi} \\   \\ \text{CH}_2=\text{C} \\   \\ \text{CH}_3 \end{array}$	---	80:20 <sup>(a)</sup>	70
	14-crown-4	81:19 <sup>(a)</sup>	70
$\begin{array}{c} \text{OTMS} \\   \\ \text{CH}_2=\text{C} \\   \\ \text{CH}_3 \end{array}$	TiCl <sub>4</sub>	85:15	84
	SbF <sub>5</sub>	89:11	quantitative
	SnCl <sub>4</sub>	86:14	quantitative
	ZrCl <sub>4</sub>	82:18	85
	BF <sub>3</sub> ·OEt <sub>2</sub>	88:12	65
	ZnCl <sub>2</sub> <sup>(b)</sup>	81:19	51

(a) Rates of equilibration of the aldol products was investigated. Under the conditions of reaction negligible equilibration took place.

(b) Reaction conducted at 25 °C.

Table 1

<u>Reagents</u>		<u>Diastereomer Ratio</u>	<u>Yield %</u>
<u>Nucleophile</u>	<u>Catalyst</u>	<u>erythro-threo</u>	
$\text{CH}_2=\text{C} \begin{array}{l} \text{OLi} \\ \text{C(CH}_3\text{)}_3 \end{array}$	--	82:18 <sup>(a)</sup>	85
	14-crown-4	81:19 <sup>(a)</sup>	85
$\text{CH}_2=\text{C} \begin{array}{l} \text{OTMS} \\ \text{C(CH}_3\text{)}_3 \end{array}$	TiCl <sub>4</sub>	99:1	50
	SbF <sub>5</sub>	98.5 : 1.5	51
	SnCl <sub>4</sub>	97.5 : 2.5	78
	ZrCl <sub>4</sub>	97.5 : 2.5	73
	BF <sub>3</sub> ·OEt <sub>2</sub>	95:5	60
	ZnCl <sub>2</sub> <sup>(b)</sup>	95:5	50

(a) Rates of equilibration of the aldol products was investigated. Under the conditions of the reaction negligible equilibration took place.

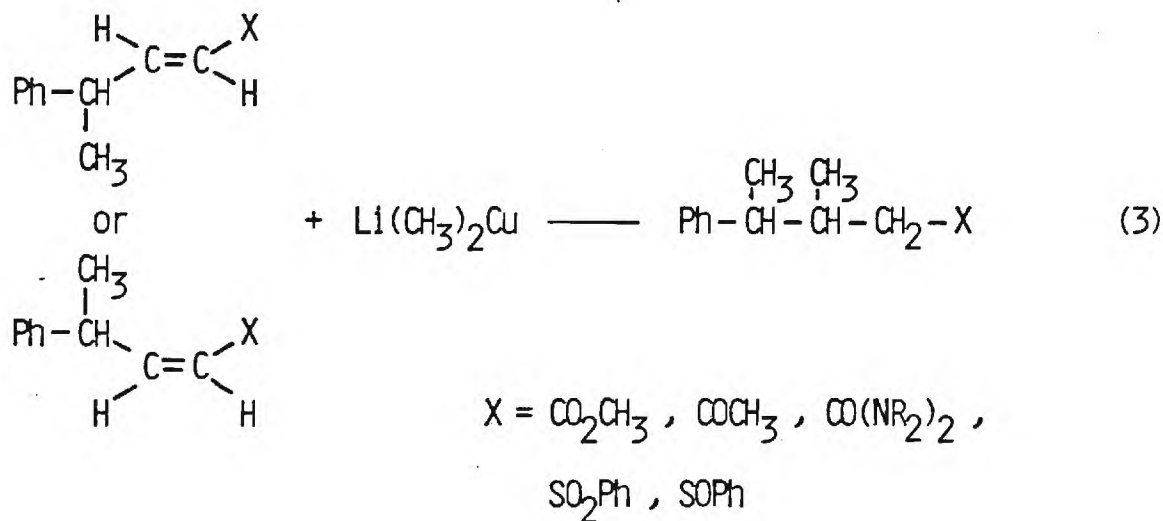
(b) Reaction conducted at 25 °C.



not substantially change the state of aggregation<sup>6</sup> or the diastereoselectivity of the lithium enolated.

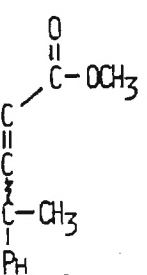
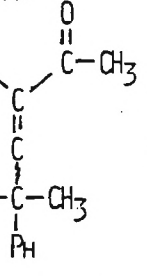
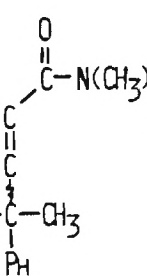
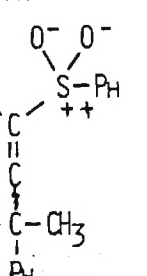
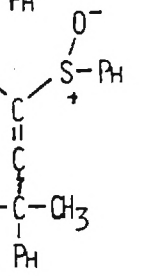
(b) Under the conditions of Lewis acid catalysis, the use of  $\text{SnCl}_4$  consistently produced higher yields of aldol product accompanied by reasonable diastereomeric ratios.

(3) A series of cis- and trans- $\gamma$ -chiral activated ethylenes have been synthesized in our laboratories and reacted with lithium dimethylcuprate (Equation 3). The activating groups include esters, ketones, and amides.



The stereochemical results of the conjugate addition reactions are summarized in Table 3. The proposed trajectory model predicts that in the comparison of these particular cis- and trans-isomers of activated double bonds containing  $\gamma$ -chiral substituents, Michael addition reactions would proceed with only modestly greater asymmetric induction for the cis-isomer as compared with the isomeric trans-compound. The results listed in Table 3 are consistent with these predictions. The cis-sulfoxide and cis-sulfone did not react with lithium dimethylcuprate although a variety of conditions were attempted. This was unfortunate since the trajectory model predicts that these activating functionalities should show the greatest difference between the cis and trans-isomers. Rousch and Lesur<sup>7</sup> have reported that in the conjugate addition of lithium dimethylcuprate to carbohydrate derived enones and  $\gamma,\beta$ -unsaturated esters, the stereochemical outcome is independent of the geometry of the starting alkene system. It must be emphasized that their systems contained alkoxy substituents at the chiral carbon. Trajectory calculations with regard to the effect of an alkoxy substituent located at the chiral carbon have been carried out by us. The results reveal that the alkoxy group at a chiral carbon appears to improve both the  $\theta$  and  $\phi$  trajectory angles (smaller  $\theta$  and a  $\phi$  closer to the chiral carbon). As a consequence, it is not surprising that the systems of Rousch and Lesur produced excellent asymmetric induction for both the cis- and trans-isomers. Heathcock et al<sup>8</sup> have reacted cis- and trans- $\gamma$ -chiral enone systems with allylsilane in the presence of Lewis acids. Reasonable diastereoselectivities were achieved with all the

TABLE 3

	R = H		R = CH <sub>3</sub>	
	<u>cis</u> (e)	<u>trans</u> (e)	<u>cis</u> (e)	<u>trans</u> (e)
	6.18:1.00 5.4:1.00 (a)	3.21:1.00	5.74:1.00	3.45:1.00
	3.25:1.00 4.53:1.00 (a) 2.94:1.00 (a)	2.91:1.00	3.01:1.00	3.11:1.00
	2.39:1.00	2.00:1.00	2.14:1.00	2.08:1.0
	(c)	1.70:1.00	(d)	(d)
	(c)	2.70:1.00	(d)	(d)

(a) Reaction conducted in the presence of triphenylphosphine.

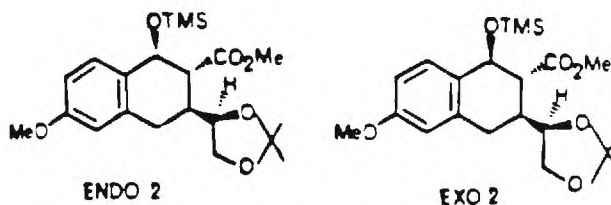
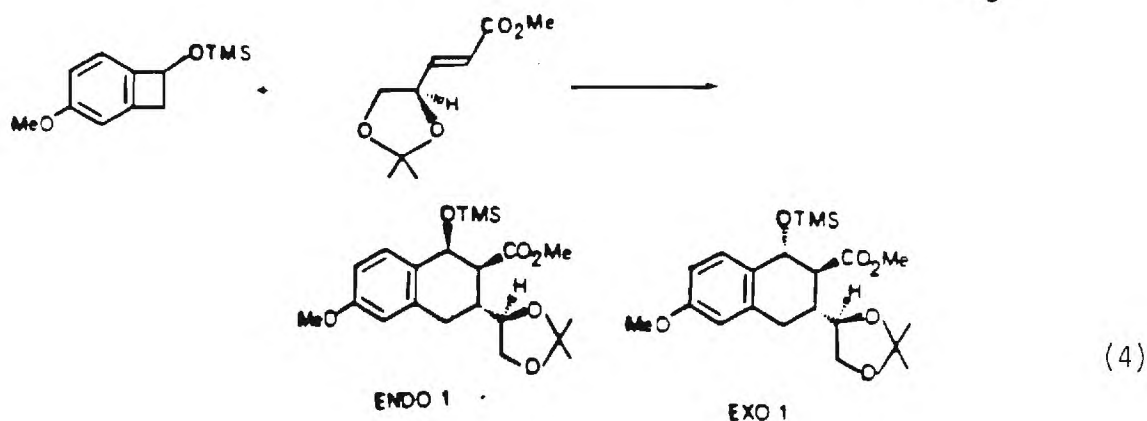
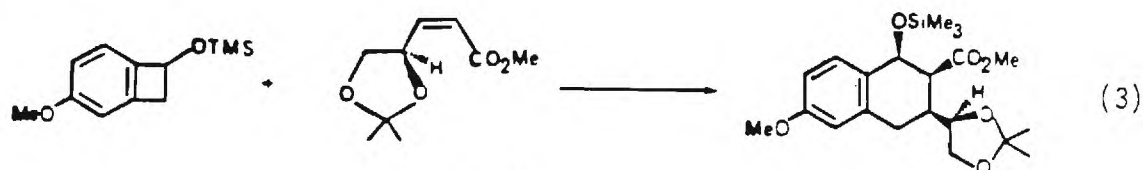
(b) Reaction conducted in the presence of BF<sub>3</sub>·OEt<sub>2</sub>.(c) The cis-isomers have been prepared but no reaction take place with lithium dimethylcuprate under a variety of conditions.

(d) These isomers have not as yet been synthesized.

(e) No cis-trans isomerization takes place during the reaction.

trans-isomers. This is consistent with the more negative  $E_N$  for the allylsilane and with the use of acid-catalysis. The stereochemical results with respect to their cis-enone system were puzzling. A chelated cyclic intermediate was postulated to explain the results.

- (4) The trajectory model predicts that as the charge at the attacking nucleophilic center decreases, the electrostatic contribution to the overall trajectory gets smaller and  $\theta$  approaches  $0^\circ$ . As a consequence, the cis- and trans-isomers of R-methyl-4-(2,2-dimethyl-1,3-dioxolanyl)-2-propenoate have been synthesized and used as dieneophiles toward the ring opened product of 1-trimethylsiloxy-5-methoxy-benzocyclobutane. Since the major frontier interaction in this [4+2] cycloaddition is that between the LUMO of the dieneophile with the HOMO of the diene, the diene can be conceptualized as a nucleophile. The transition state can thus be visualized as truncated to reflect the nucleophile character of the diene. Since the charge associated with the leading bond forming terminus of the diene is very small, the trajectory model predicts a  $\theta$  smaller than that predicted for the lithium dimethylcuprate reactions. Reaction of the cis- isomer (Equation 3) resulted in the formation of one adduct as 95% of the reaction mixture. In order to confirm the stereochemistry a single X-ray analysis was conducted on this product. In contrast to this result, the trans- isomer produced four "major" products: the two endo adducts and the two exo adducts each in 2.2:1.0 ratio (Equation 4).



The results are in agreement with the predictions of the trajectory model.

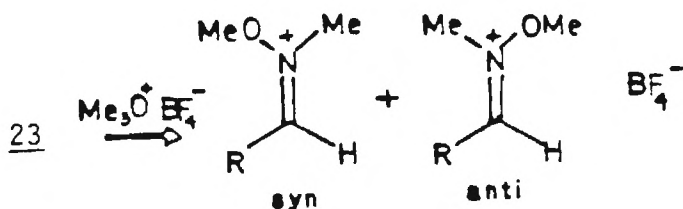
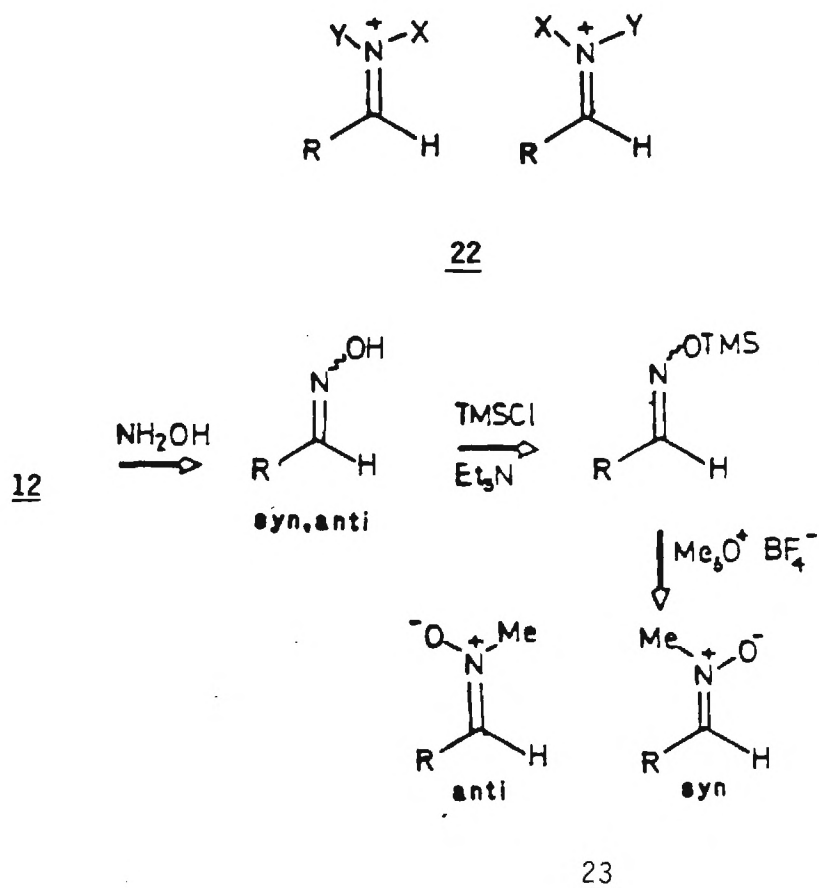


Proposed Research - Experiment

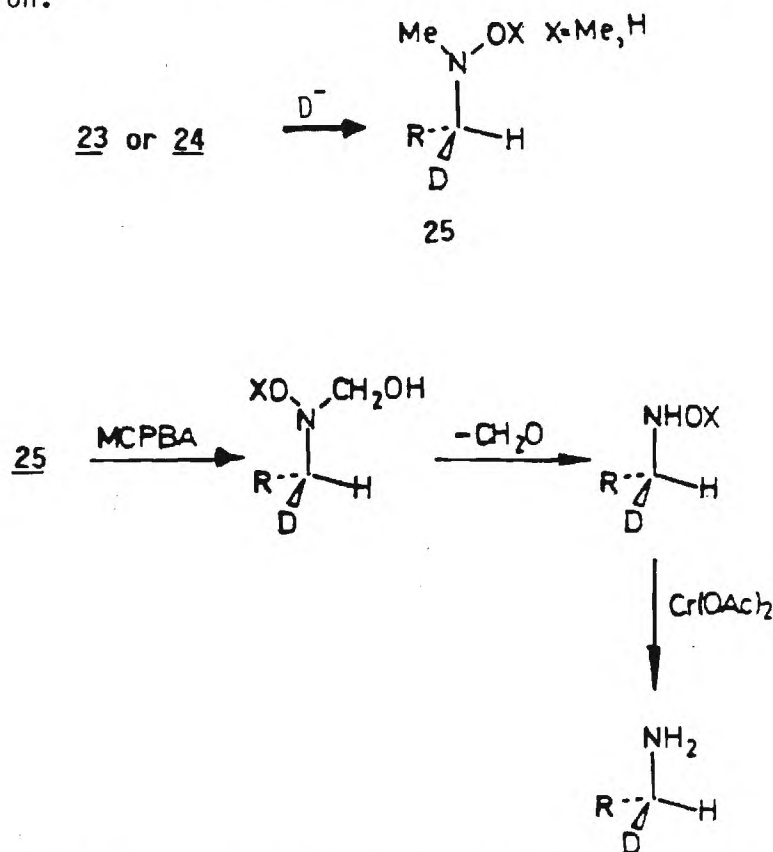
The previous section outlines the pertinent features and predictions of the proposed trajectory model. Details of the theory may be found in Appendices A, B, C and D. A limited body of experimental data derived from the work conducted in our laboratories, as well as from the laboratories of others, provides support for the model.

Asymmetric Induction in the Reaction of Nucleophiles with Model Lewis Acid Catalyzed Systems

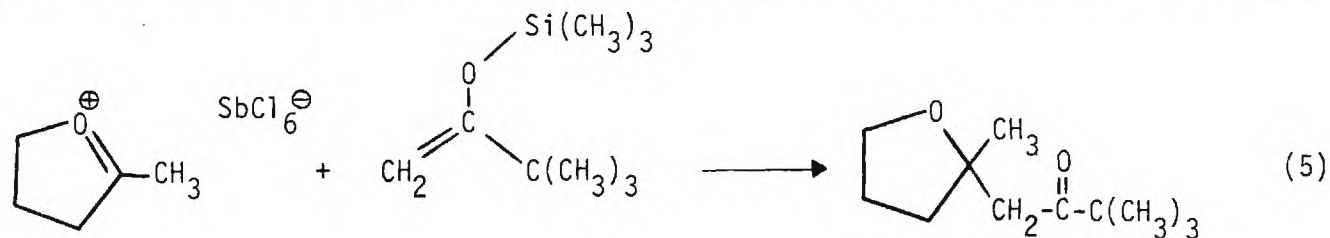
In order to investigate the degree of asymmetric induction with respect to the variation of angle  $\phi$ , the iminium systems, 22, provide a model for Lewis acid catalysis with a defined stereochemistry.



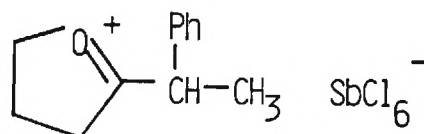
The N-X and N-Y bonds must differ enough in energy to create an unsymmetrical  $\sigma$  and  $\sigma^*$  density to the C-N plane normal to the plane of the molecule and thus direct  $\phi$  to a particular quadrant. This will either increase or decrease the degree of induction as a function of the stereochemistry of 22. In order to substantiate this effect, it is proposed to stereospecifically prepare the two possible  $\pi$ -electrophiles, 23 and 24 as shown<sup>12</sup>. Addition of nucleophiles such as  $\text{CH}_3\text{Li}$ ,  $\text{CH}_3\text{MgX}$ , allylsilanes, or allylstannane<sup>38</sup> will be employed to investigate the degree of asymmetric induction. The substituted hydroxylamine products, 25 may be converted to a mixture of diastereoisomeric amines via oxidation and subsequent reduction.<sup>14</sup>



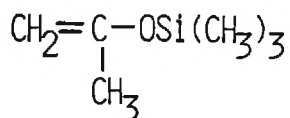
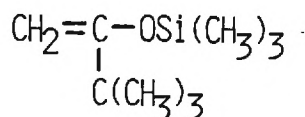
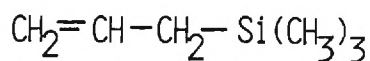
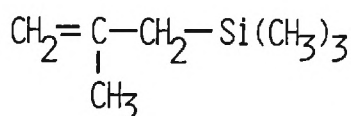
Alternate approaches to control the disposition of the Lewis acid with respect to the substituents attached to the carbonyl carbon are being pursued in our laboratories. 2-Methyl-1-oxonia-1-cyclopentene hexachloroantimonate<sup>16</sup> has been reacted with the silyl enol ether of pinacolone (Equation 5). 3,3-Dimethyl-1-



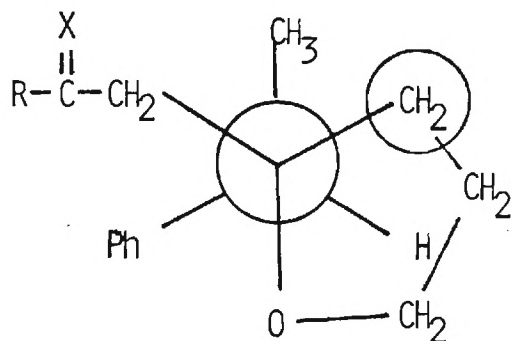
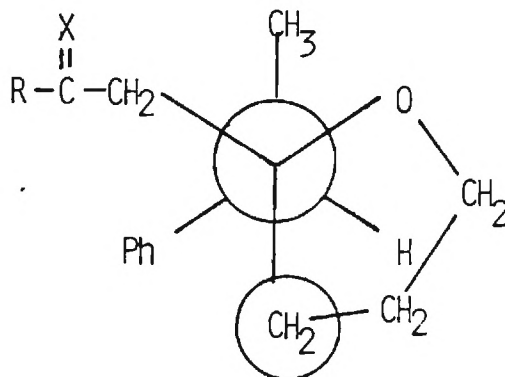
[2-(2-methyletetrahydrofuran)]-2-butane was produced in reasonable yields.<sup>15</sup> In this example, the Lewis acid is built into the molecule and the cyclic nature of the species dictates its stereochemistry with respect to the rest of the system. As a continuation of the study, it is proposed to synthesize the following  $\alpha$ -chiral species by methods similar to those used to prepare 28

28

and to investigate the magnitude of asymmetric induction accompanying reaction with the following nucleophiles:

29303132

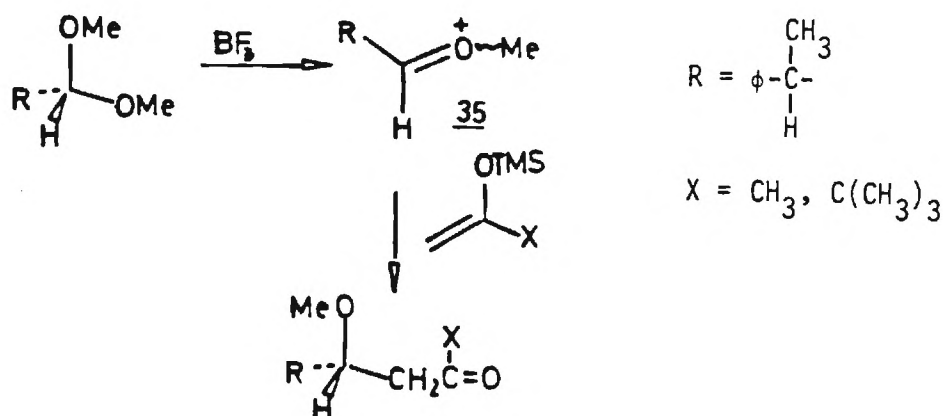
Molecular models indicate that the most stable conformation of the two diastereomeric products are those shown in structure 33 and 34.

3334

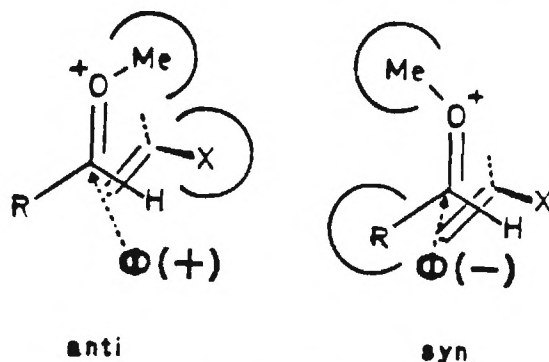
The ratio of diastereomers will be determined by means of NMR techniques and if need be a single crystal X-ray analysis. The shielding environment of the phenyl substituent should cause the circled methylene protons in structure 33 to absorb further upfield as compared to the counterparts in structure 34.



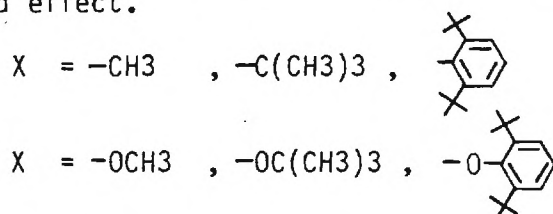
Another proposed experiment dealing with this subject involves the  $\alpha$ -chiral acylium ion, 35, whose preparation is illustrated as follows:



Assuming that 35 may adopt either a syn or anti  $\text{R}-\text{CH}_3$  configuration in the reaction with an enol derivative, the two transition states which develop are:

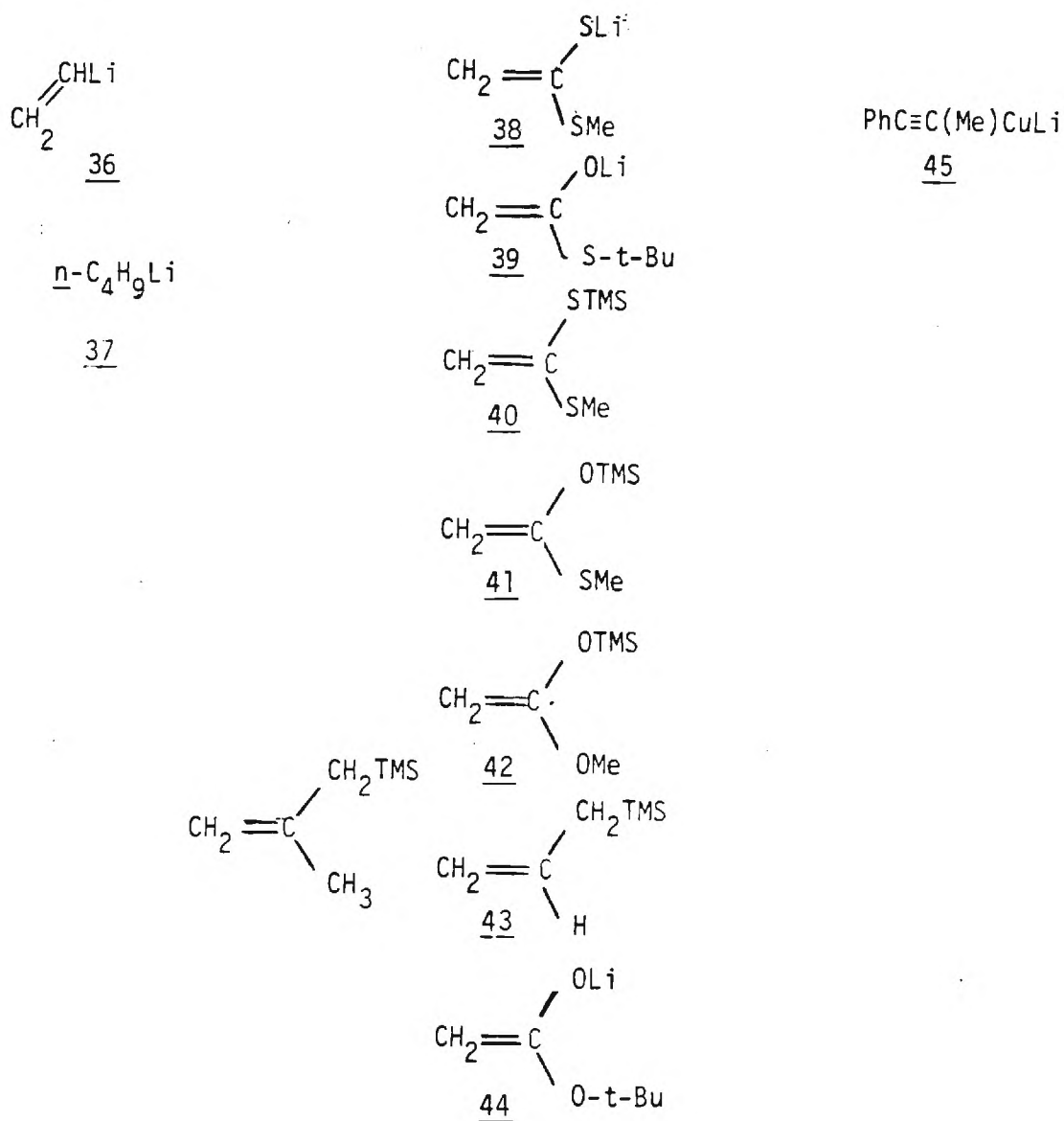


Each of these has an angle  $\phi$  in different quadrants. Thus, the syn-transition state leads to greater asymmetric induction than the anti counterpart. The syn alignment is destabilized by the constant  $\text{CH}_3-\text{R}$  steric interaction while the anti congener has a destabilizing  $\text{X}-\text{OCH}_3$  interaction. Therefore, the degree of asymmetric induction is a function of the steric bulk of  $\text{X}$  within the same transition state geometry. It is proposed to investigate the reactions of 35 with the silylenol ethers in the following series in order to substantiate the postulated effect.

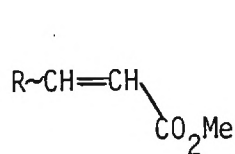
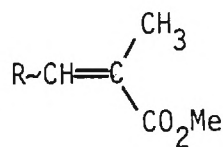
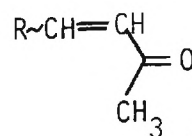
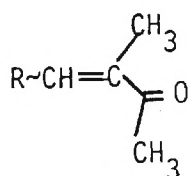
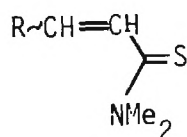
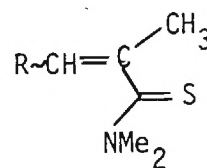
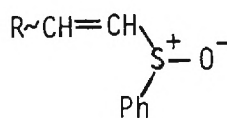
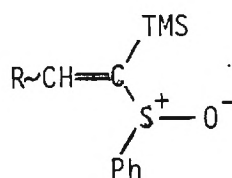
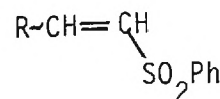
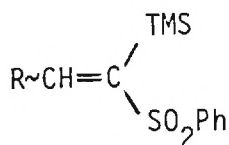
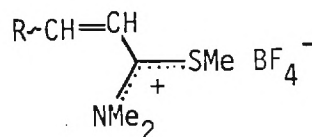
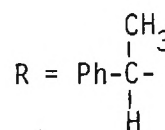


# Asymmetric Induction in the Conjugate Addition of Nucleophiles to $\alpha$ -Chiral Activated Ethylenes

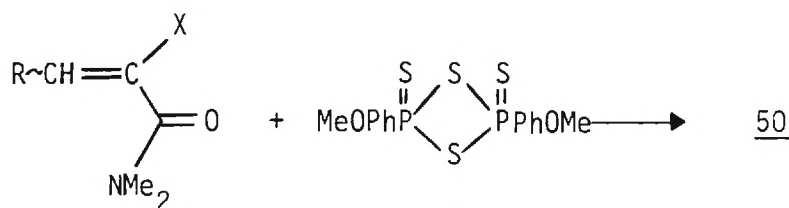
The trajectory model predicts that asymmetric induction accompanying conjugate addition to cis- and trans  $\gamma$ -chiral  $\alpha,\beta$ -unsaturated esters, ketones and dialkylamides should be modestly greater for the cis-isomer as compared to the trans. This is indeed the case with regard to their reaction with lithium dimethylcuprate. It has been emphasized that when the activating group is a thioester, a sulfone, or a sulfoxide, the model predicts that the cis-isomer will exhibit substantially greater asymmetric induction as compared to the trans-isomer. Attempts were made to conjugatively add lithium dimethylcuprate to the cis- and trans  $\gamma$ -chiral sulfoxides and sulfones (Table 3). While addition was successful for the trans-isomers, no reaction conditions could be found which would allow addition of the cuprate to the cis-isomers. It would be a presumption to suggest that one incomplete series of cuprate reactions validates the proposed trajectory model. As a consequence, it is proposed to expand the study of asymmetric induction accompanying conjugate addition of the following series of nucleophiles:



to the following series of  $\gamma$ -chiral conjugated  $\pi$ -electrophiles

4647484950515253545556

The carbonyl derivatives 46 to 49 are available from Wittig or thione methyllide chemistry and have already been synthesized to our laboratories.<sup>17,18</sup> Synthesis of the acrylamide by the same procedures<sup>20</sup> and conversion to the corresponding thiocarbonyl derivative with 58 should be straightforward.<sup>19</sup> Alkylation of 50 gives 56. The synthesis of all remaining  $\alpha,\beta$ -unsaturated  $\pi$ -electrophiles have been successfully synthesized in our laboratories.<sup>21</sup>



X=H, Me

5857

The trajectory model predicts that as the  $E_N$  of the nucleophile becomes more negative, the value of  $\theta$  approaches  $0^\circ$ . This, of course, would be accompanied by greater asymmetric induction. The nucleophiles listed above (36-45) represent a systematic variation in  $E_N$ . It must be realized, however, that varying states of aggregation of the organometallic species would certainly effect the relative  $E_N$  values. A recent theoretical investigation of organocuprates suggest a planar dimer structure and that the alkyl-ligands in lithium dimethylcuprate have a higher HOMO than in 45.<sup>22</sup> Any prediction of the stereoselectivity of lithium dimethylcuprate vs. 45 will not be possible - only experimental information will reveal this.

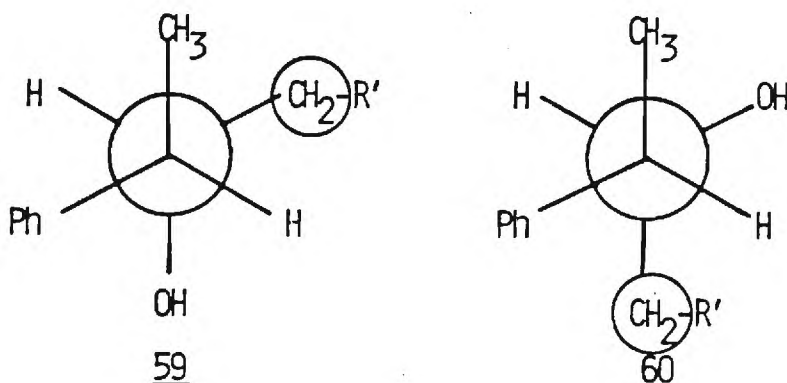
Table 4 summarizes the reported work dealing with conjugate addition of the nucleophile 36 through 45 with activated double bonds. In the cases listed, the activated alkenes do not possess  $\gamma$ -chiral substituents.<sup>37</sup>

Table 4

$\pi$ -Electrophile	Nucleophile	Reference
$\text{CH}_2=\text{CH}-\text{C}(=\text{O})\text{R}$	38	23
	39	24
	$\text{LiCu}(\text{CH}_3)_2$	25, 26
	45	36
$\text{CH}_2=\text{CH}-\text{C}(=\text{O})\text{O}^+\text{ER}$	41	24
	42	27
	43	28
	$\text{LiCu}(\text{CH}_3)_2$	35
$\text{CH}_2=\text{CH}-\text{C}(=\text{O})\text{OR}$	$\text{LiCu}(\text{CH}_3)_2$	26
	45	26
$\text{CH}_2=\text{CH}-\text{C}(=\text{S})\text{NR}_2$	36	29
	37	29
	45	30
$\text{CH}_2=\text{C}(\text{SCH}_3)\text{S}^+\text{O}^-\text{R}$	43	31
$\text{CH}_2=\text{C}(\text{CO}_2\text{CH}_3)\text{S}^+\text{O}^-\text{R}$	$\text{LiCu}(\text{CH}_3)_2$	32
$\text{CH}_2=\text{C}(\text{TMS})\text{SO}_2\text{R}$	37	33
$\text{CH}_2=\text{CH}-\text{SO}_2\text{R}$	$\text{LiCu}(\text{CH}_3)_2$	34

Using Table 4 as a basis, it is proposed to investigate as many chemically realizable permutation of reaction partners as possible in order to provide support for the theoretical prediction presented earlier.

Assignment of the stereochemistry to the diastereoisomers produced from addition of the various nucleophiles to the  $\pi$ -electrophiles is relatively easily accomplished using 300 MHz NMR spectroscopy provided that both diastereoisomers are available. Herein lies an important reason why the above chiral R group was selected. The shielding properties of the phenyl in R allows differentiation of the two possible diastereomers via the upfield shift of the group gauche (circled) to the phenyl in the rotomers determined to be the most important conformation for each of the diastereomers. (59 and 60). In the cases in which three asymmetric centers require correlation, single crystal X-ray crystallography would be most useful.



#### Asymmetric Induction in the Reaction of Unsymmetrical Allyl Anion Derivatives with $\alpha$ -Chiral Aldehydes-Asymmetric Induction as a Function of Regiochemistry

The trajectory model suggests that, for a given  $\pi$ -electrophile, the larger the HOMO coefficient ( $C_{\text{PN}}$ ) and the smaller the charge ( $q_{\text{N}}$ ) at the nucleophilic center, the smaller the angle  $\theta$  and associated ambident ions such as unsymmetrical allyl anions represent ideal systems to test this hypothesis since both the HOMO coefficient and the charge are different at the two nucleophilic centers while the HOMO energy is held constant (Figure 4).

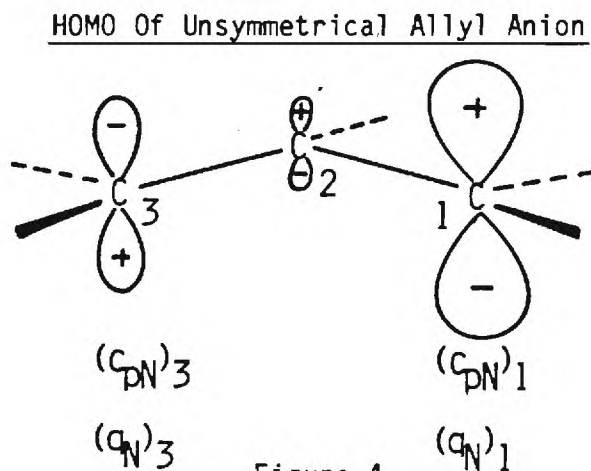


Figure 4

Allyl metal and related systems have found wide application in organic synthesis. Indeed, there is considerable literature concerning the generation and regiochemical reactions of unsymmetrical allyllithium derivatives with a wide variety of electrophiles.<sup>39</sup> In contrast, much less has been reported for unsymmetrically substituted allylpotassium and allylcesium. By analogy with studies concerning the state of aggregation of benzyl lithium, allyllithium should be monomeric in diethyl ether and tetrahydrofuran.<sup>40</sup> Theoretical calculations<sup>41</sup> indicate that solvent free allyl lithium is a symmetrical species ( $C_{2v}$  symmetry) while NMR studies using isotopic perturbation techniques suggest in tetrahydrofuran solution allyllithium is an unsymmetrical  $\pi$ -structure with similar, but not identical  $C^1Li$  and  $C^3Li$  bond lengths.<sup>42</sup> Allyl potassium, using the same techniques, was found to be a symmetrical  $\pi$ -structure. Barriers to rotation about the carbon-carbon bonds of allylalkali metal compounds in THF have been measured by NMR exchange rates of the terminal allyl protons:  $\Delta G^\ddagger$ , kcal/mol (coalescence temp.,  $^\circ C$ ), =  $10.7 \pm 0.2$  ( $-51^\circ$ ) for allyllithium,  $16.7 \pm 0.2$  ( $-51^\circ$ ) for allylpotassium, and  $18.0 \pm 0.3$  for allylcesium.<sup>43</sup> The NMR data has been interpreted to mean that as the alkali metal ion becomes larger, the allyl anion becomes less shielded electrostatically.

Table 5 summarizes the results of semi-empirical molecular orbital calculations carried out in our laboratories on a series of 1-substituted allylanions. The parameters used to describe the allyl anion geometry<sup>44</sup> are illustrated in Figure 5.

Geometric Parameters for Allyl Anion

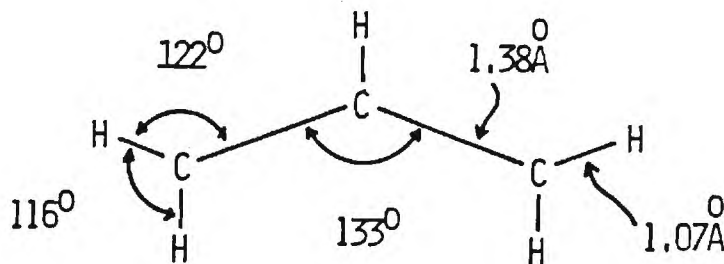
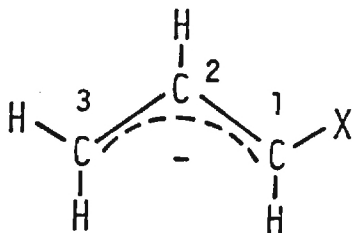


Figure 5

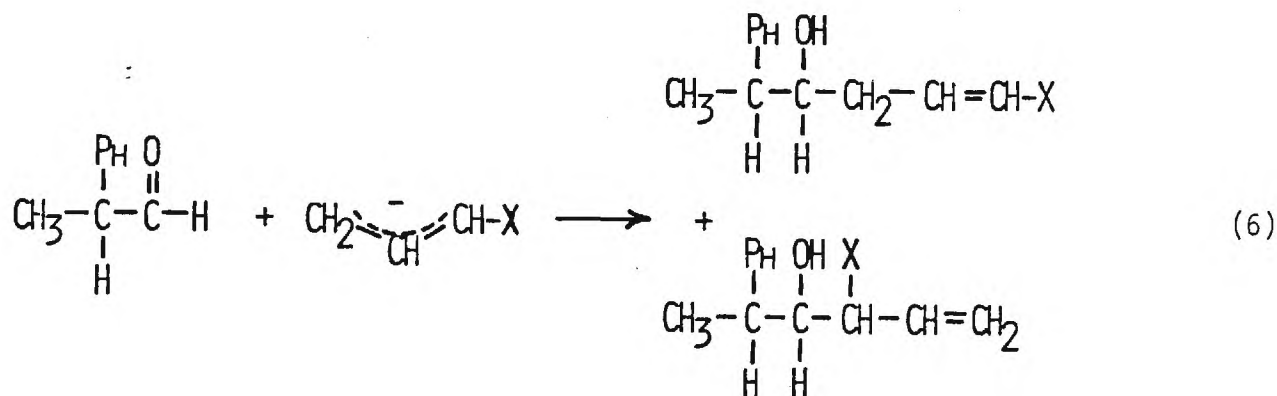
Table 5 summarizes the magnitude of the HOMO coefficients and charges associated with the terminal carbons of an unsymmetrical allyl anion substituted at the 1-position with electron-donating and electron withdrawing substituents. Thus, for an oxygen-substituted allylanions, the trajectory model predicts that in the



Table 5. MNDO Calculations on Unsymmetrical Allyl Anions.

X	$C_{p1}$	$q_1$	$C_{p3}$	$q_3$	$E_N(\text{ev})$
-F	0.702	-0.353	0.679	-0.463	-1.010
-Cl	0.714	-0.395	0.680	-0.443	-1.389
-OR	0.689	-0.409	0.676	-0.488	-0.615
-SR	0.698	-0.426	0.683	-0.462	-0.992
-NR <sub>2</sub>	0.660	-0.326	0.671	-0.511	-0.184
-CH <sub>3</sub>	0.708	-0.550	0.678	-0.460	-0.999
-CHO	0.688	-0.493	0.618	-0.360	-2.136
-NO <sub>2</sub>	0.681	-0.389	0.602	-0.298	-3.011
-CN	0.700	-0.440	0.663	-0.384	-1.977

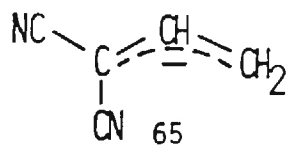
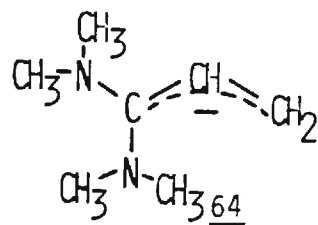
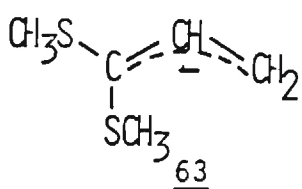
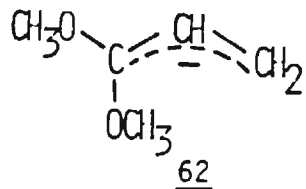
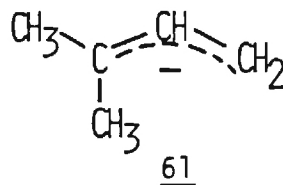
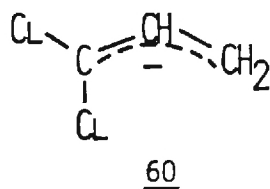
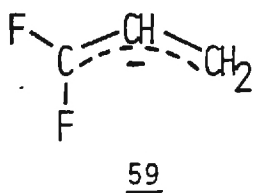
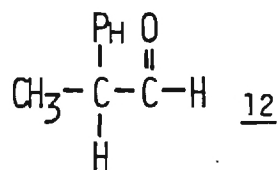
reaction with an  $\alpha$ -chiral aldehyde, the products resulting from attack at the 1-position should show greater diastereoselectivity than the corresponding attack at the 3-position (Equation 6). In a similar manner predictions with regard to



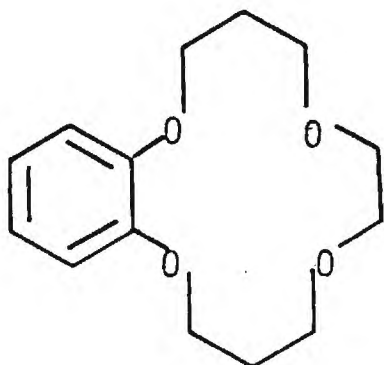
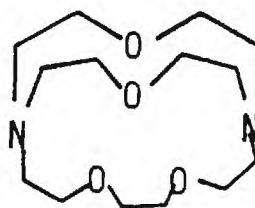
diastereoselectivity can be made for each of the substituted allyl anions listed in Table 5. It should be emphasized that the calculations were performed on solvent free-cation free anions. Incorporation of a lithium countercation decreases the HOMO energy by approximately 5-6 ev's. In general, the more associated the cation with the allyl anion the more negative the HOMO energy. The relative magnitudes of the coefficients and charges do not appear to change in the presence of a metal cation symmetrically disposed with respect to the terminal position of the anion. It has already been stated that as the HOMO energy becomes more negative,  $\theta$  approaches  $0^\circ$ . Thus, according to Table 5, electron-withdrawing substituents attached to the allyl anion should show greater diastereoselectivity than the corresponding anions substituted with electron-donating substituents. Since the allyl metal system approaches the free anion as the size of the alkali metal cation increases, it would be anticipated that the magnitude of the diastereoselectivity would decrease as one proceeds from an allyllithium to an allylpotassium to an allylcesium. In a similar manner, the magnitude of the diastereoselectivity should also decrease when an allyllithium is complexed with a macrocyclic or macrobicyclic multidentate ligand.

Proposed Research - Experimental

It is proposed to investigate the regioselectivity and the diastereoselectivity resulting from the reaction of  $\alpha$ -chiral aldehyde 12 with unsymmetrical allyl anions 59 to 65.



In order to gain a better understanding of the relationship between regioselectivity, diastereoselectivity and the degree of "nakedness" of the allyl anion, lithium, potassium and cesium will be employed as the counter cations in these studies. In addition, TMEDA, as well as macrocyclic ligands 66 and 67, will be used in conjunction with the allyl lithium derivatives in order to solvate and separate the lithium cation from the allyl anion.<sup>45,46,47</sup>

6667

For reference purposes, several related unsymmetrical allyl lithium compounds, their precursors and their methods of generation are summarized in Table 6. Included in Table 6 is the precedent for the production of significant yields of the two regioisomers using non-chiral carbonyl quenching agents. The allyl lithium derivatives in Table 6 are not appropriate at this juncture for the study of diastereoselection since reaction at the position alpha to the hetero substituent will lead to products with three contiguous chiral centers. This would necessitate analysis of mixtures containing four diastereomers. Coupled with the fact that there are two regioisomeric products, the analysis would become intractable. In contrast to this, the use of allyl anions 59 through 65 would produce product distributions which would be easily susceptible to analysis by NMR.

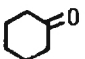
The preparation of the lithium salts of anions 59,<sup>48</sup> 60,<sup>49</sup> and 62,<sup>50</sup> and their subsequent reactions with a variety of non-chiral electrophiles have been reported in the literature. Anions of analogous structure to 61,<sup>39</sup> 63,<sup>39</sup> 64,<sup>39</sup> and 65,<sup>51</sup> have been reported. As a consequence, no difficulty is anticipated in the generation of these anions. The potassium and cesium salts will be generated from the hydrocarbon precursors using trimethylsilylmethylpotassium and trimethylsilylmethylcesium, respectively.<sup>52</sup>

A critical factor in the proposed study is that both regioisomeric products must be produced in quantities large enough to be observed and analyzed with available tools (NMR). It has been demonstrated that structural variations in the carbonyl quenching agent produces dramatic changes in the regiochemical product distribution. It is conjectured that the regiochemical distribution of products is related to the reduction potential of the carbonyl compound. Nevertheless, based upon the spectrum of quenching agents reported in Table 6, chiral aldehyde 12 represents an excellent candidate for obtaining both regiochemical products.

Table 6

Allyl Anion Precursor	Method of Anion Generation	$\pi$ -Electrophile	Products and Ratios		Yields	Ref.
$\begin{array}{c} R \\ \diagup \\ N-CH_2-CH=CH_2 \\ \diagdown \\ R \end{array}$	$\text{sec-C}_4\text{H}_9\text{Li}$ (2 eq), THF, -78° then -10°, 2 hr	$\begin{array}{c} O \\    \\ \text{Cyclohexyl}-C-H \end{array}$	$\begin{array}{c} R \\ \diagup \\ N-CH-CH=CH_2 \\ \diagdown \\ R \end{array}$	$\begin{array}{c} R \\ \diagup \\ N-CH_2-CH=CH-R \\ \diagdown \\ R \end{array}$		53
		$\text{C}_6\text{H}_5\text{CHO}$	50	50	64	
		$\text{CH}_3\text{COCH}_3$	46	54	48	
		$\text{C}_6\text{H}_5\text{COCH}_3$	43	57	59	
		$\begin{array}{c} O \\    \\ \text{Cyclohexyl}-C \end{array}$	40	60	74	
			45	55	71	
<hr/>						
$(\text{C}_6\text{H}_5)_3\text{PbCH}_2\text{-CH=CCl}_2$	$n\text{-C}_4\text{H}_9\text{Li}$ , THF, -90°, 20 min	$\text{C}_2\text{H}_5\text{CHO}$ -90°, 5 min	$R\text{-CCl}_2\text{-CH=CH}_2$ 69	$R\text{-CH}_2\text{-CH=CCl}_2$ 28	97	49
$\text{CH}_2=\text{CH-CHCl}_2$	LDA, THF, -78°, 2 hr	$\text{C}_6\text{H}_5\text{COCH}_3$ -90°, 5 min then $(\text{CH}_3)_3\text{SiCl}$	29	18	47	
<hr/>						
$\text{C}_6\text{H}_5\text{CHO}$ , $\text{CH}_3\text{COCH}_3$ and cyclohexanone gave only one regioisomer.						
$R'O\text{-CH}_2\text{-CH=CH}_2$	$\text{sec-C}_4\text{H}_9\text{Li}$ , THF, -65°		$\begin{array}{c} R'O-CH-CH=CH_2 \\   \\ R \end{array}$	$R'O\text{-CH}_2\text{-CH=CH-R}$		54
$R'=\text{CH}_3, \text{C}_2\text{H}_5$	10 min	$\begin{array}{c} CH_3 \\   \\ CH-C-H \\   \\ CH_3 \end{array}$	32	68	99	
		$\begin{array}{c} O \\    \\ \text{Cyclohexyl}-C \end{array}$	28	72	93	

Table 6 (continued)

Allyl Anion Precursor	Method of Anion Generation	$\pi$ -Electrophile	Products and Ratios		Yields	Ref
$\text{CH}_2=\text{CH}-\text{CH}_2-\text{NO}_2$	$\underline{n}\text{-C}_4\text{H}_9\text{Li}$ , THF  -80° to -90°		$\text{O}_2\text{N}-\underset{\text{R}}{\text{CH}}-\text{CH}=\text{CH}_2$	$\text{O}_2\text{N}-\text{CH}_2-\text{CH}=\text{CH}-\text{R}$		
		$\underline{t}\text{-C}_4\text{H}_9\text{CHO}$	52	48	65	55
		$\underline{n}\text{-C}_5\text{H}_{11}\text{CHO}$	56	44	76	
		$\text{C}_6\text{H}_5\text{CHO}$	30	70	74	
			50	50	82	
$\text{C}_6\text{H}_5\text{Se}-\text{CH}_2-\text{CH}=\text{CH}_2$	LDA, THF -78°, 10 min	$\text{C}_6\text{H}_5\text{COCH}_3$	$\text{C}_6\text{H}_5\text{Se}-\underset{\text{R}}{\text{CH}}-\text{CH}=\text{CH}_2$ 15	$\text{C}_6\text{H}_5\text{Se}-\text{CH}_2-\text{CH}=\text{CH}-\text{R}$ 85	-	56
$\underline{1}\text{-C}_3\text{H}_7\text{S}-\text{CH}_2-\text{CH}=\text{CH}_2$	$\underline{\text{sec}}\text{-C}_4\text{H}_9\text{Li}$ , ether, -78°C, then 30° 30 min	$\text{C}_6\text{H}_5\text{CHO}$	$\underline{1}\text{-C}_3\text{H}_7\text{S}-\underset{\text{R}}{\text{CH}}-\text{CH}=\text{CH}_2$ 28	$\underline{1}\text{-C}_3\text{H}_7\text{S}-\text{CH}_2-\text{CH}=\text{CH}-\text{R}$ 72	-	57



The relationship between diastereoselectivity and regioselectivity could alternately be explored with allyl anions of the type shown in Figure 6 where

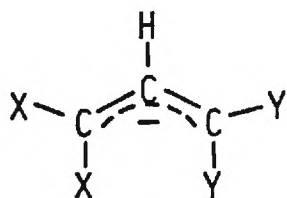
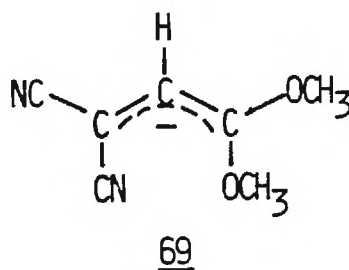
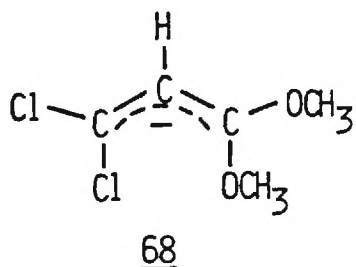


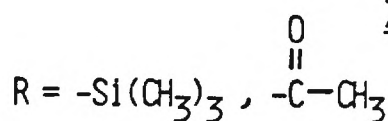
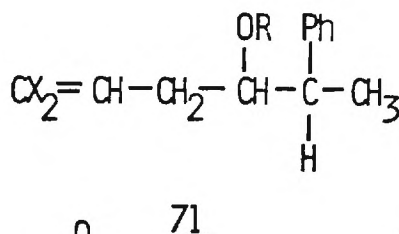
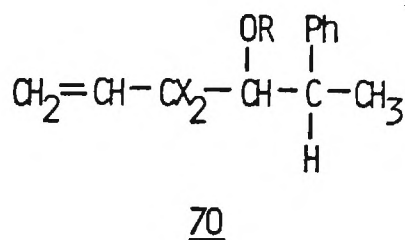
Figure 6

perturbation by a "wisely chosen" Y substituent would effect the regiochemical distribution of products. In addition, greater stability may be imparted to the anion with the correct choice of Y. Semi-empirical molecular orbital calculations (MNDO) would be extremely valuable in guiding the choice of Y. Some illustrative examples would be 68 and 69.

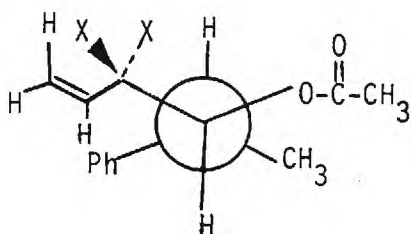
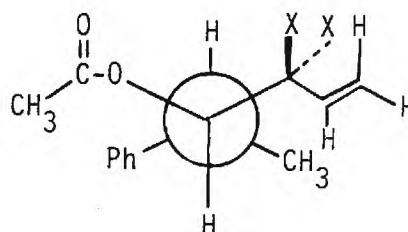


In the process of investigating the regioselectivity and diastereoselectivity in the reactions of unsymmetrical allyl anions, factors such as temperature, solvent and concentration of organometallic reagent will be held constant in order to facilitate consistent theoretical interpretation.

The products will be analyzed as their trimethylsilyl and acetyl derivatives (70 and 71).<sup>49</sup> The ratio of regioisomers and the ratio of 70 to 71



will be determined primarily by NMR techniques. The two regioisomers are easily distinguished from each other on the basis of  $^1\text{H}$  NMR. For instance,  $\phi\text{CH}(\text{OH})\text{CH}_2\text{-CH=CCl}_2$ , the product of reaction of the 1,1-dichloroallylanion with benzaldehyde, has an NMR spectrum which shows the  $\text{CH}_2$  protons as two doublets ( $J_1 = 6.5$  Hz;  $J_2 = 7.0$  Hz) at 2.40 ppm and vinyl proton as a triplet ( $J_1 = 6.5$  Hz) at 5.75 ppm. In contrast, the product obtained from reaction with acetone,  $(\text{CH}_3)_2\text{C}(\text{OH})\text{CCl}_2\text{-CH=CH}_2$ , shows its vinyl protons as an ABC multiplet (3d of d) at 5.25-6.60 ppm.

7273

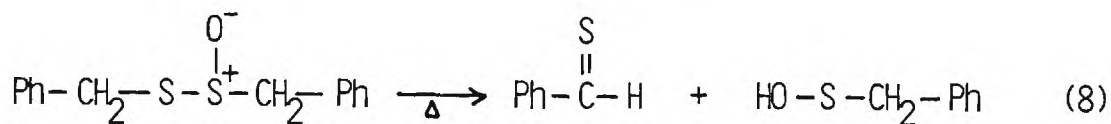
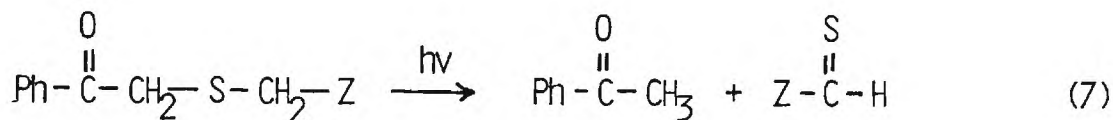
The relative stereochemistry of the two diastereomers will be assigned on the basis of NMR chemical shifts. Heathcock et al.<sup>5</sup> have stated that "acyclic compounds having vicinal stereocenters, each bearing one hydrogen, normally exist predominantly in the conformation having hydrogens anti, so as to minimize gauche interactions." The pertinent conformations of the products derived from the reaction of unsymmetrical allyl anions 59 to 65 with  $\alpha$ -chiral aldehyde 12 are shown in structures 72 and 73. The chemical shift of the internal vinyl hydrogen of 72 should be in the shielding environment of the vicinal phenyl group and should resonate further upfield than the corresponding vinyl hydrogen in 73. Conversely, the acetyl methyl of 73 should be in the shielding environment of the vicinal phenyl and should be upfield with respect to the corresponding methyl group in 72.

#### Asymmetric Induction in [4+2] Cycloaddition Reactions of Dienes with $\alpha$ -Chiral Thioaldehydes

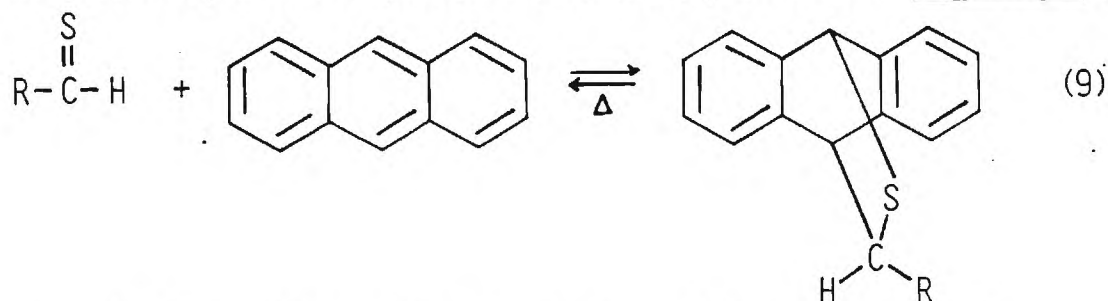
[4+2] Cycloaddition reactions provide facile means of constructing six-membered rings. In particular, a wide variety six-membered heterocycles have been synthesized using this methodology.<sup>58,59</sup>

Thiocarbonyl compounds undergo [4+2] cycloaddition reactions at temperatures ranging from  $-78^\circ$  to  $160^\circ$  depending on the substituents attached to the thiocarbonyl functionality. Of the wide variety of known thiocarbonyl compounds, thioaldehydes are, in general, the most reactive. This high reactivity results in both positive and negative components of the reaction. While it is true that cycloadditions occur readily, the occurrence of concurrent polymerization processes has, until recently, limited investigation into the chemistry of this

interesting functional group. Vedejs<sup>60,62,63</sup> and Baldwin<sup>61</sup> have developed methods for in situ generation of thioaldehydes by photochemical and thermal processes, respectively (Equations 7 and 8). An important fact has emerged with respect to the thermal generation of



the alkyl thiosulfinate. It has been demonstrated that, under the reaction conditions, the sulfenic acid formed regenerates more alkylthiosulfinate. Baldwin has trapped the thioaldehyde with anthracene and used the adduct to thermally generate the thioaldehyde in the presence of a variety of dienes (Equation 9).



Both of these methods should provide convenient and efficient means of generating  $\alpha$ -chiral thioaldehydes in the presence of dienes from readily synthesized precursors.

In general, thiocarbonyl groups are more reactive than carbonyl groups in [4+2] cycloaddition reactions. This is easily understood in terms of frontier molecular orbital theory. Figure 7 attempts to display the relative energy levels of the carbonyl and thiocarbonyl functionalities in relationship to a diene. The calculated vacant  $\pi_{\text{C}=\text{S}}$  molecular orbital for thioformaldehyde is 2.8 eV. lower in energy than that calculated for  $\pi_{\text{C}=\text{O}}$  for formaldehyde.<sup>62</sup> The filled  $\pi_{\text{C}=\text{S}}$  molecular orbital is calculated to be 3 eV. high in energy than that calculated for  $\pi_{\text{C}=\text{O}}$ . The energy difference between the HOMO of the diene and  $\pi_{\text{C}=\text{S}}^*$  ( $\Delta E_2$ ) is much smaller than the corresponding energy difference involving  $\pi_{\text{C}=\text{O}}$  ( $\Delta E_1$ ).

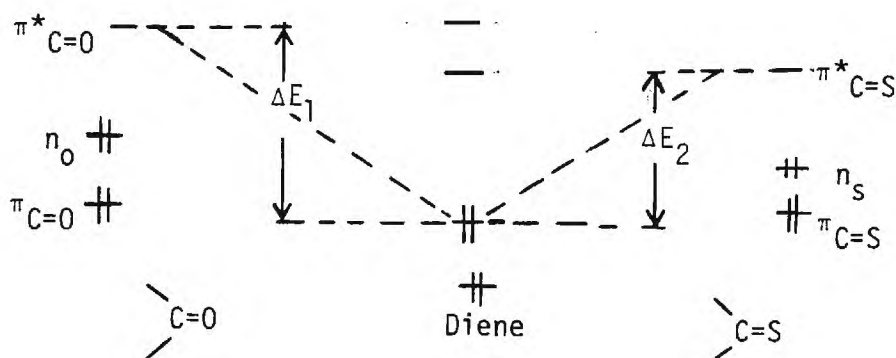


Figure 7

Since these relative energy differences are, to a first order approximation, related to the relative rates of reaction, it becomes evident why thiocarbonyls are more reactive.

In the presence of a Lewis acid the energy picture for the carbonyl in Figure 7 is somewhat altered. Complexation of the Lewis acid with the non-bonding electron pair on the oxygen leads to a lowering of the  $\pi^*$  energy level thus decreasing the magnitude of  $\Delta E_1$  and increasing the rate. Lewis acid catalyzed cycloaddition reactions of carbonyls have been investigated.<sup>64-68</sup> In fact, asymmetric induction accompanying the reactions of dienes with a variety of  $\alpha$ -chiral aldehydes have been reported.

Basic to the above theoretical analysis is the recognition that the major frontier interaction is that between the HOMO of the diene and the LUMO of the dieneophile. This implies that the diene behaves as the nucleophile and the dieneophile as the  $\pi$ -electrophile. Using this view of the reaction, the trajectory model (outlined in Appendix A, B, C and D) has been invoked to analyze approach trajectories toward aldehydes, aldehydes complexed with  $BF_3$ , and thioaldehydes. The results are summarized in Table 7. In this analysis only the orbital components of the trajectory model (charge transfer and repulsion) are considered since the charge associated with the leading bond-forming terminus of the diene is extremely small. The smaller the charge, the smaller the contribution of the electrostatic component of the model. In the extreme, when the charge of the nucleophilic component is zero, the electrostatic contribution vanishes.

Analysis of Table 7 reveals that  $BF_3$  catalyzed nucleophilic attack at the carbonyl group of acetaldehyde has a larger  $\theta$  ( $68^\circ$ ) than that of thioacetaldehyde ( $50.9^\circ$ ) and that the  $\phi$  for thioacetaldehyde ( $+25.6^\circ$ ) is in the quadrant containing the methyl substituent while the  $\phi$  for the  $BF_3$ -acetaldehyde is approximately  $0^\circ$ . Thus, if the methyl substituent were replaced by a chiral group, the model predicts that the  $\alpha$ -chiral thioaldehyde would show greater diastereoselectivity than the acid-catalyzed aldehyde counterpart.

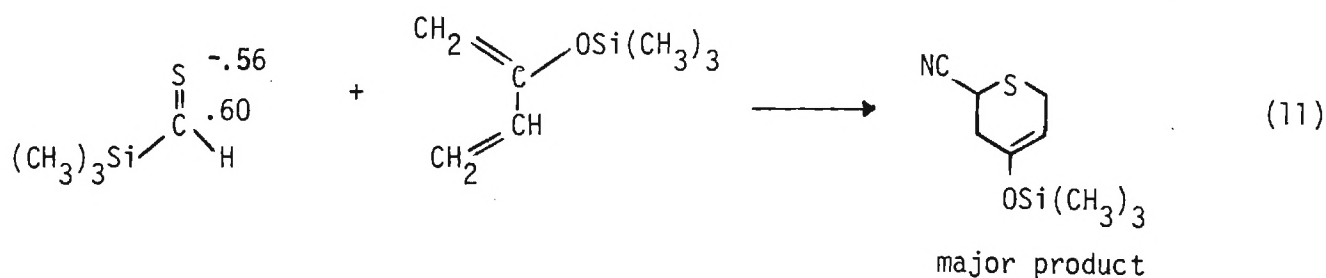
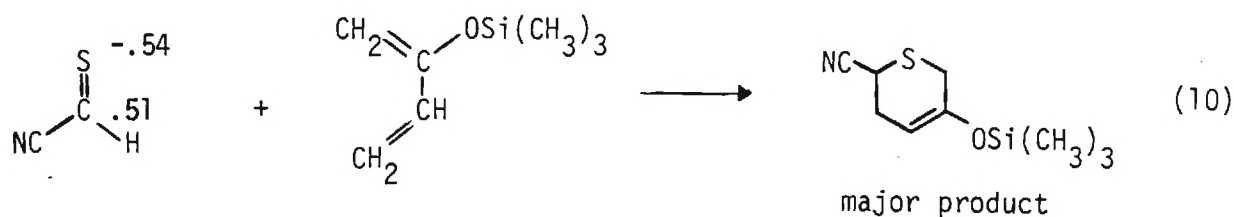
The major frontier interaction in describing the regiochemistry accompanying the cycloaddition of thioaldehydes with electron-rich dienes is the  $\pi_{CS}^*$  (LUMO) -  $\pi_{CC}$  (HOMO) interaction. Equations 10 and 11 reveal the effect of electron withdrawing and electron-donating substituent attached to the thioaldehyde

Table 7

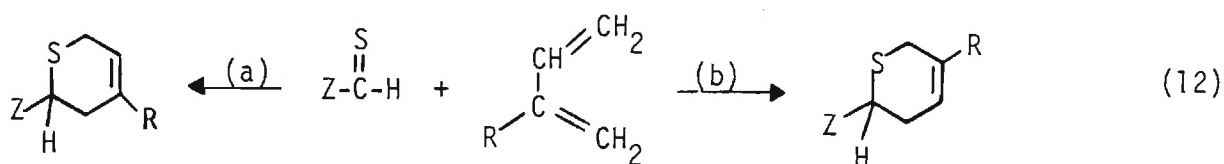
	Attraction		Repulsion		Resultant Orbital	
	$\theta$	$\phi$	$\theta$	$\phi$	$\theta$	$\phi$
$\begin{array}{c} \text{O} \\ \parallel \\ \text{CH}_3 - \text{C} - \text{H} \end{array}$	60.2	-13.4	75.4	-18.3	67.8	-15.9
$\begin{array}{c} \text{O}^+ - \text{BF}_3^- \\ \parallel \\ \text{CH}_3 - \text{C} - \text{H} \end{array}$	67.3	-35.1	57.4	+14.1	62.4	-10.5
$\begin{array}{c} \text{BF}_3^- - \text{O}^+ \\ \parallel \\ \text{CH}_3 - \text{C} - \text{H} \end{array}$	74.2	+3.3	68.3	+19.7	71.3	+11.5
$\begin{array}{c} \text{S} \\ \parallel \\ \text{CH}_3 - \text{C} - \text{H} \end{array}$	63.1	+22.6	38.6	+28.2	50.9	+25.6
Nucleophile Distance	$E_N$		$E_{PN}$		$q_N$	
2.00 Å	-8.0		.5		-.5	

68° | 0°

functionality. It may be seen that the observed regiochemistry is consistent with the relative magnitude of the coefficients at carbon and sulfur in  $\pi^*_{CS}$ .



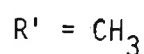
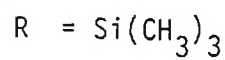
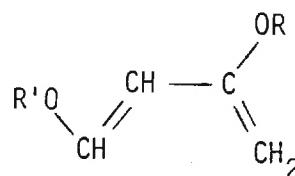
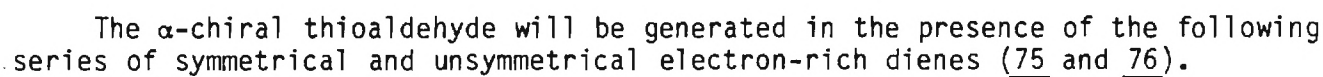
Thus, electron withdrawing substituents favor pathway (a) while electron-donating substituents favor pathway (b) (Equation 12).<sup>62</sup>



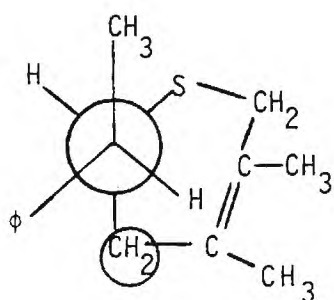
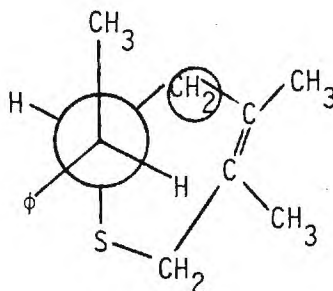
### Proposed Research - Experimental

It is proposed to synthesize  $\alpha$ -chiral thioaldehyde 74 as outlined in the following reaction sequences by procedures similar to these in the literature.<sup>69-72</sup>

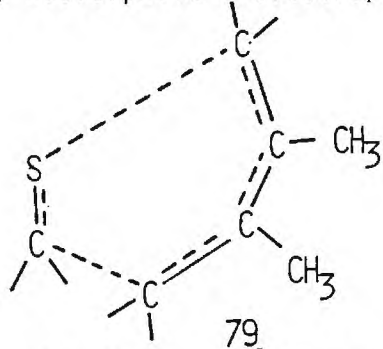
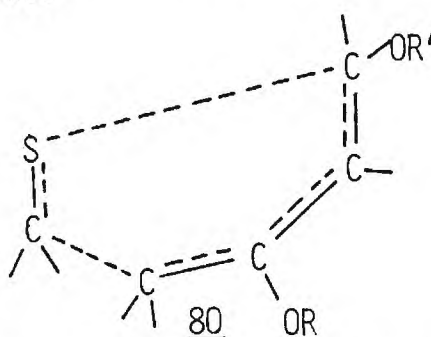




There is **no** regiochemistry associated with the reaction of diene 75 with thioaldehyde 74. The diastereoselectivity accompanying the cycloaddition reaction may be determined using high resolution NMR techniques. Employing the "Heathcock postulate"<sup>5</sup> structures 77 and 78 would represent the dominant conformations of the two diastereoisomers which would be possible from the reaction.

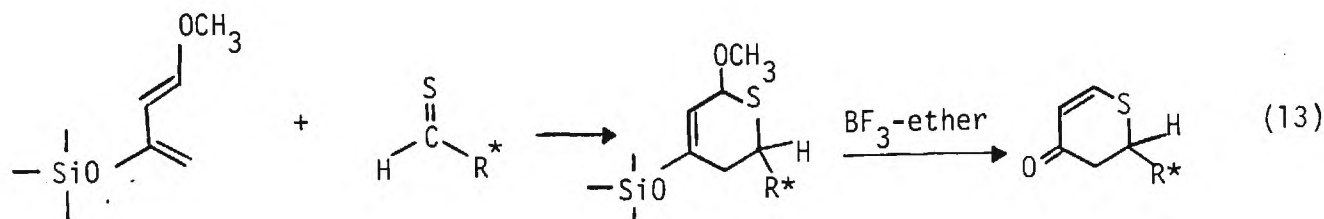
7778

The circled methylene protons of structure 77 should be observed further upfield than corresponding methylene protons of structure 78 because of the shielding effect of the proximate phenyl substituent. MNDO calculations on the  $\alpha$ -chiral thioaldehyde employed in the proposed investigation indicate that the  $\pi^*_{cs}$  coefficients at carbon and sulfur are substantially different. ( $c_{\pi^*C} = 0.69$  and  $c_{\pi^*S} = -0.56$ ). As a consequence it would be anticipated that reaction with a symmetrical diene such as 2,3-dimethyl-1,3-butadiene would proceed through a transition state which is slightly truncated (79). In other words, the nucleophilic component is somewhat greater than the electrophilic component in the transition state. It must be emphasized that the proposed trajectory model deals with only nucleophile  $\pi$ -electrophile interactions.

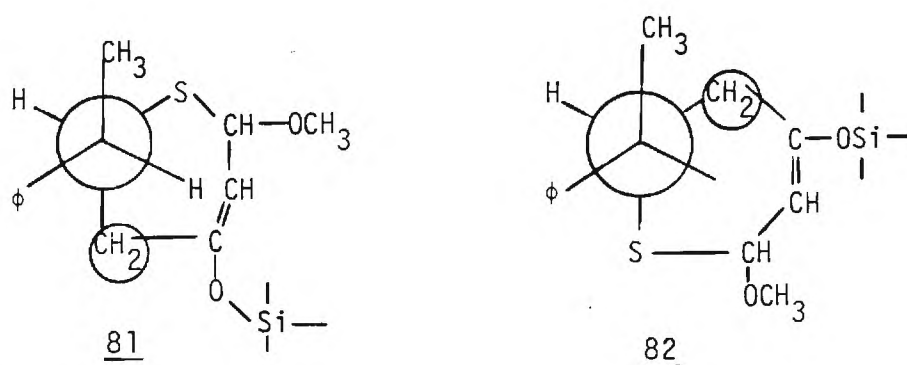
7980

Thus, in order to augment the nucleophilic component of the total interaction, it is important to choose a diene which produces a greatly truncated transition state. Within the language of frontier molecular orbital theory, the  $\pi^*_{cs}$  LUMO- $\pi_{CC}$  HOMO interaction must be greatly dominant. This may be easily accomplished by employing Danishefsky diene 80 since the coefficient associated with C1 of the diene is twice the magnitude of that associated with C4 hence producing the truncated-transition state. Thus, the diene resembles a nucleophile and the thiocarbonyl component the  $\pi$ -electrophile. As a result it is anticipated that

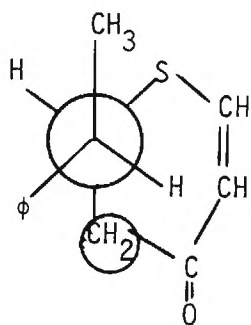
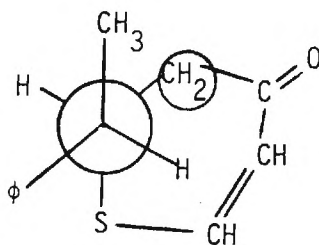
only one regioisomer will be formed (> 90%) (Equation 13). In addition, molecular models indicate that the exo transition state will be lower energy than the



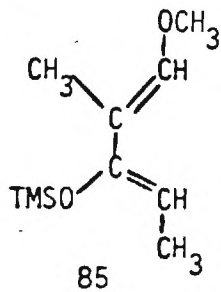
corresponding endo transition state. Figures 81 and 82 represent the most important conformations of the diastereomeric products of the major regioisomer. As in the case dealing with 2,3-dimethyl-1,3-butadiene, these



diastereomers may be easily distinguished using NMR techniques. The methylene protons circled in structure 81 should appear upfield from the corresponding protons in structure 82 due to the shielding effect of the proximate phenyl group. If, in fact, both the exo and endo transition states compete effectively, then analysis of the initial cycloadduct would be complicated due to the presence of cis and trans-isomers at the methoxymethylene position. If such a circumstance arises the initial products will be reacted with  $\text{BF}_3 \cdot \text{Et}_2\text{O}$  by the Danishefsky procedure to produce the corresponding enones for subsequent NMR analysis. Figures 83 and 84 represent the most important conformations of the enone products. Again, NMR analysis of the product mixture would provide the ratio of diastereomers based upon the integration of the absorption of the circled methylene protons. If needed, X-ray analysis of solid derivatives of the products could be pursued if the NMR analysis is not adequate.

8384

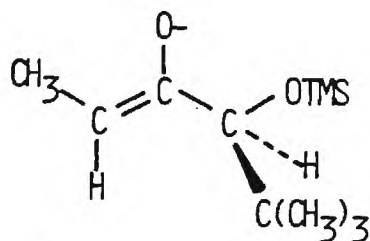
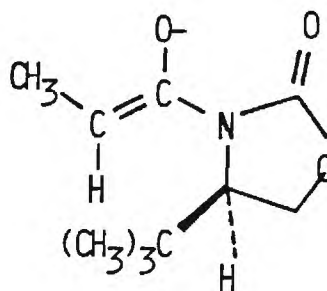
Danishefsky et al has investigated diastereoselection in the reaction of  $\alpha$ -chiral aldehydes with a variety of electron-rich dienes under Lewis acid conditions. The trajectory model predicts that  $\alpha$ -chiral thioaldehydes should show greater diastereoselection than corresponding  $\alpha$ -chiral aldehydes under Lewis acid conditions. Unfortunately, the electron-rich diene Danishefsky employed (85) was not that suggested in the proposed work<sup>68</sup>. In order to make the necessary comparison diene 76 will be reacted with 2-phenylpropanal under Lewis and conditions. Analysis of the diastereoselectivity accompany reaction will be conducted using NMR techniques similar to those previously discussed. Danishefsky has reacted the acetonide of glyceraldehyde with diene 76 as the initial step in the synthesis of compactin. The acetonide of thioglyceraldehyde will be prepared by previously discussed methods and reacted with diene 76 to ascertain the magnitude of asymmetric induction.

85

The series of experiments outlined will provide powerful data to ascertain the generality of the proposed trajectory model.

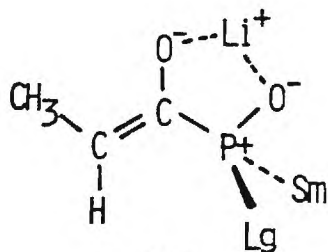
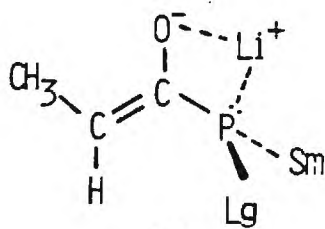
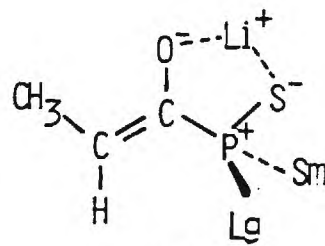
Asymmetric Induction Using Chiral Auxillary Substituents

The incorporation of chiral auxillary groups in enolate reagents represents an interesting and useful approach for maximizing diastereoselectivity and enantioselectivity. Heathcock<sup>73</sup> has elegantly shown that by employing chiral substituted enolates, such as 86, only one aldol isomer (1,2-erythro) is obtained from reaction with an  $\alpha$ -chiral aldehyde. Evans<sup>74</sup> has also demonstrated that an enolate substituted with optically active chiral auxillary groups, such as 87, give aldol products (1,2-erythro) with high optical purity with an estimated selectivity in the order of 2500:1. The great importance of this chiral auxillary to promote mutual kinetic resolution in the synthesis of natural products is obvious.

8687

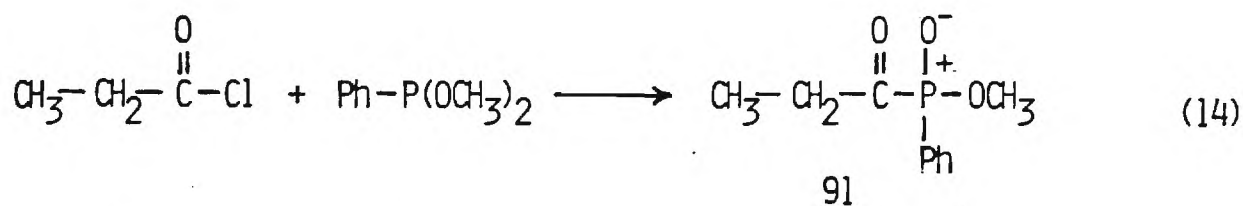
It is proposed to construct new molecules containing chiral auxillary substituents. Studies will be aimed at demonstrating comparable double stereodifferentiation to 86 or comparable enantioselection to 87. In addition, facile single step conversion of the aldol product to an ester, a methyl ketone or an aldehyde will present another possible advantage over published reagents. This latter advantage would also allow rapid synthesis of natural products derived from consecutive multiple aldol condensation sequences. Polyether ionophore antibiotics would represent such natural products.

The chiral auxillary substituted lithium enolates to be studied may be represented by 88, 89, and 90 (where Lg=large substituent and Sm=small substituent). The precursors to each of the lithium enolates (as well as the corresponding di-n-butylboron enolates) are acylphosphine oxides,<sup>75,76</sup> acylphosphines,<sup>75,76</sup> and acylphosphine sulfides which are readily available by

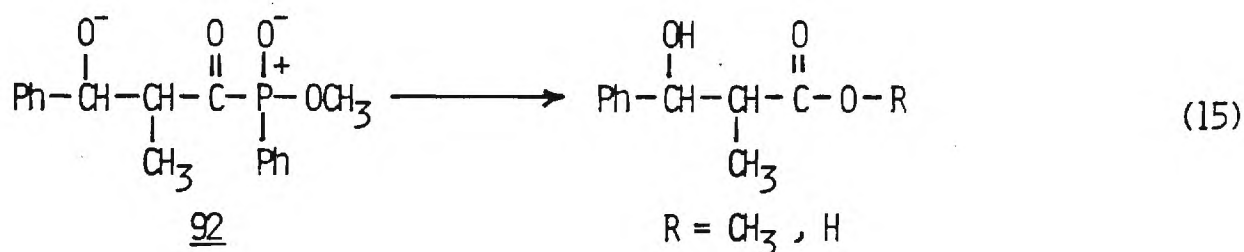
888990

published procedures. Clearly, the large phosphorus substituent in the acyl derivatives will influence the stereochemistry of the enolates which are formed upon reaction with sterically hindered bases. It is anticipated that the cis-isomers will dominate. In addition, since the lithium cation can bridge the proximate heteroatoms and lock the enolates into conformationally fixed systems, the different steric requirements of the groups attached to phosphorus (Lg and Sm) will result in dramatic face selectivity in reactions with  $\pi$ -electrophiles.

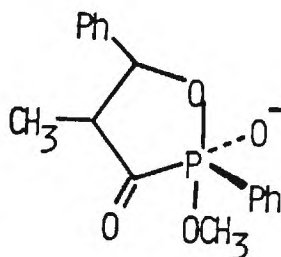
Acylphosphine oxide 91 has been synthesized in our laboratories (Equation 14) and subsequently converted to a stable lithium enolate with lithium



diisopropylamide in THF at  $-78^\circ\text{C}$ . Reaction of the enolate with benzaldehyde produced the aldol product with an erythro-threo ratio of 12:1 in 85% isolated yield. The assumed product 92 was not isolated but was readily converted to the isolated  $\beta$ -hydroxy ester or acid by simple addition of methanol or water, respectively, to the reaction mixture (Equation 15).



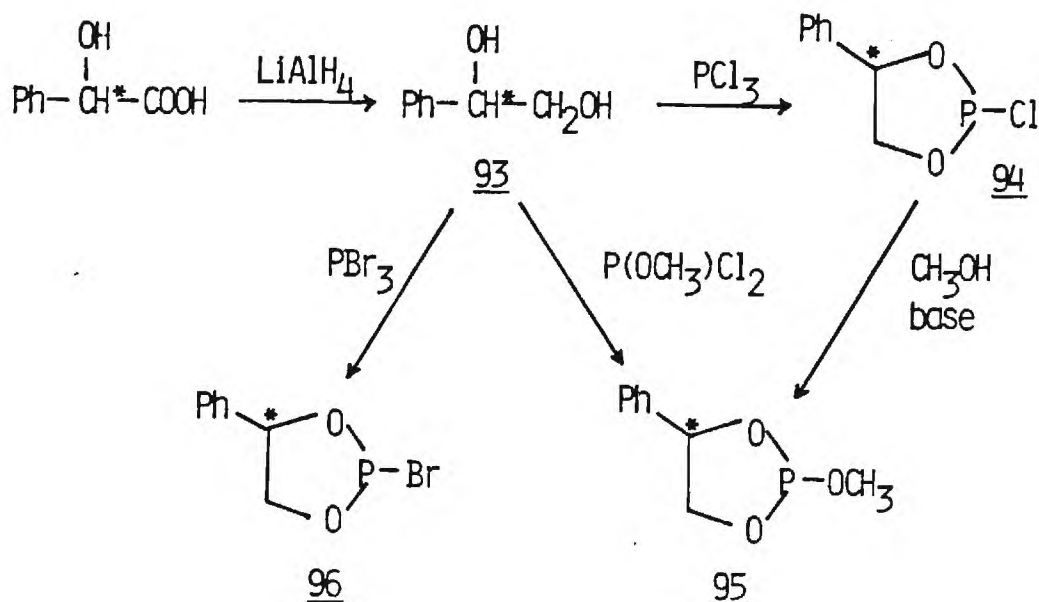
Several advantages of this aldol scheme have become apparent. The initial aldol product did not equilibrate (erythro to threo) under the reaction conditions over a period of 30 minutes at  $-78^\circ\text{C}$ . This suggests internal stabilization of the lithium alkoxide moiety possibly via the following hypervalent species. The final





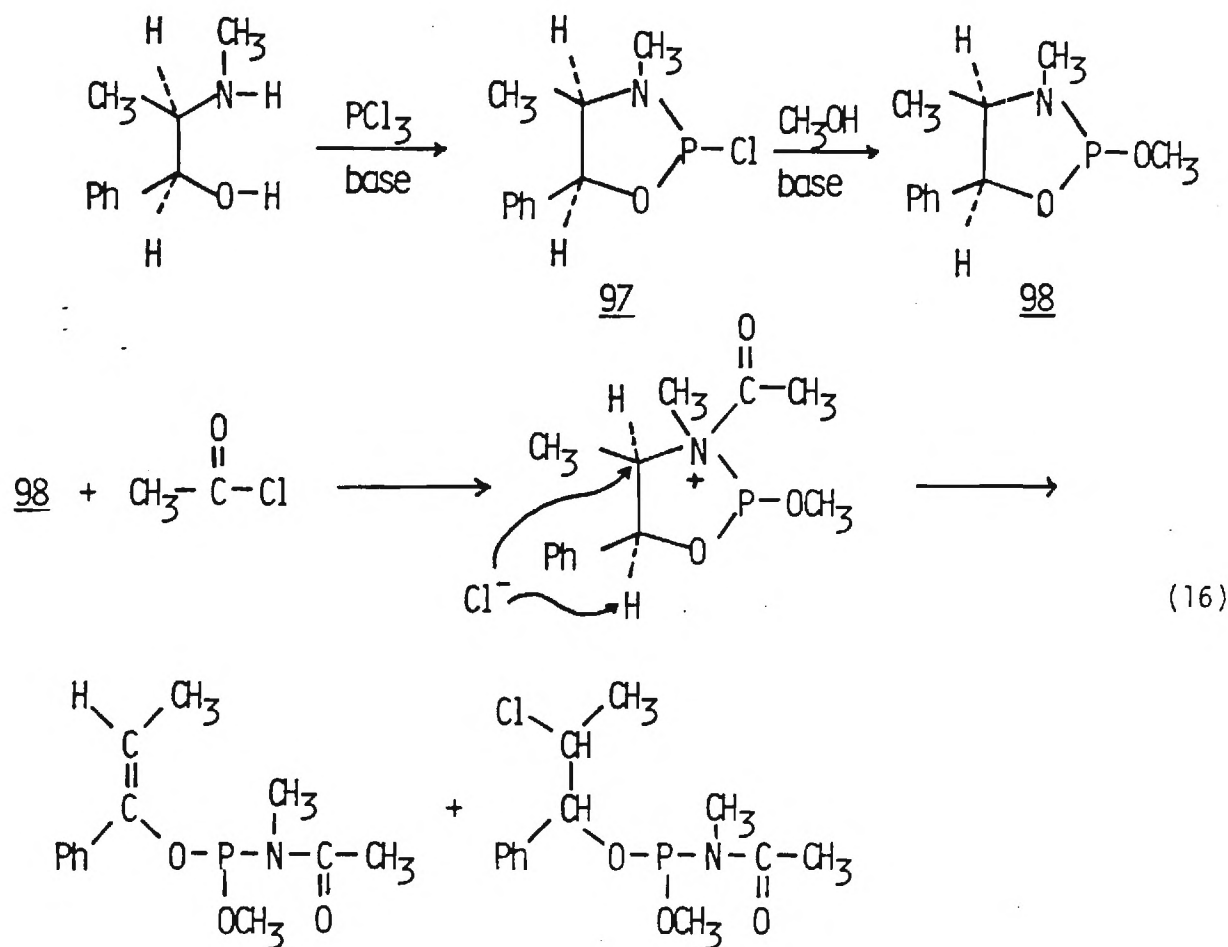
carboxylic acid or its derivative was produced on work-up under conditions which were exceedingly mild and, as such, would not effect other protecting groups which might be present in a more complex  $\pi$ -electrophile. The erythro selectivity of the enolate derived from 91 toward benzaldehyde was less than that for 87 (100:0) but far better than that for 86 (1:3.6).

In order to take full advantage of the readily available "chiral pool", the precursors to the acylphosphine oxides derived from either of the two enantiomers of mandelic acid or ephedrine have been synthesized. It was visualized that subsequent reaction with acid chlorides under Abrusov conditions would produce the optically active acylphosphine oxide. The results are summarized as follows:<sup>77,78</sup>

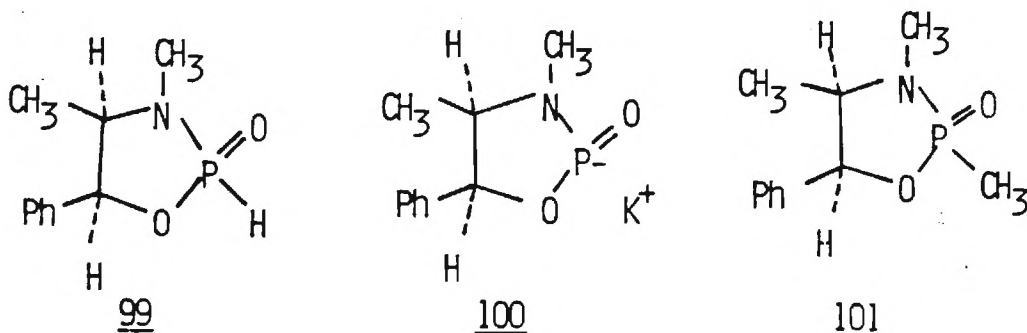


1. S- or R-Mandelic acid was reduced with lithium aluminum hydride to produce diol 93. Reaction of 93 with  $\text{PCl}_3$  followed by methanol and a tertiary amine produced cyclic phosphite 95 which was found to be a 70:30 diastereomeric mixture. Isolation and characterization of chlorophosphite 94 again revealed a 70:30 diastereomeric ratio. Clearly, in order for the resulting acylphosphine oxide (formed from the reaction of 95 and an acid chloride) to be of any value a "pure" optically active phosphite precursor is necessary. Quite surprising was the observation that reaction of diol 93 with  $\text{PBr}_3$  produced 96 as only one diastereomer. Reaction of 96 with methanol and a tertiary amine followed by reaction with acid chlorides is currently under investigation.

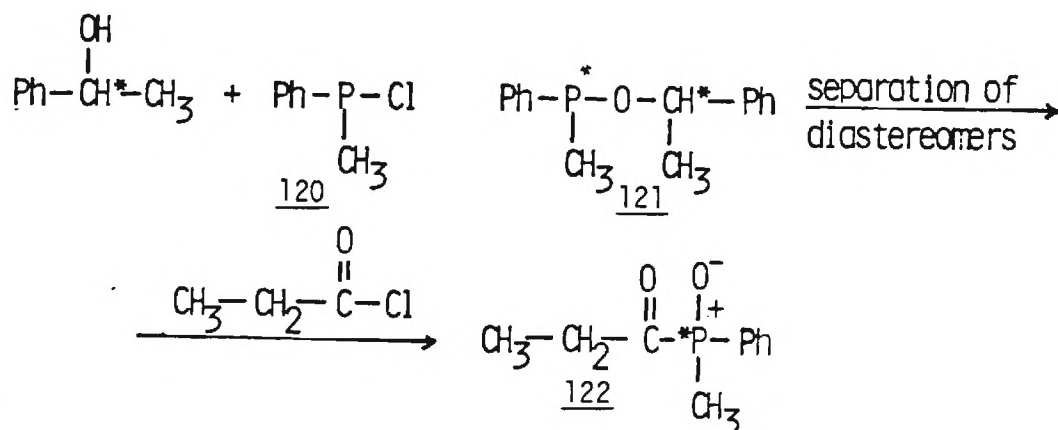
2. Reaction of (1R,2S)-(-)-ephedrine or (1S,2R)-(+)-ephedrine with  $\text{PCl}_3$  produced 97 in 87% isolated yield. Analysis using  $^1\text{H}$  NMR (300 MHz) revealed only one diastereomer. Subsequent reaction with methanol in the presence of a tertiary amine produced 98 in quantitative yield with an 88:12 diastereomeric ratio. Further investigation aimed at enhancing this ratio was abandoned when it was discovered that reaction of 98 with acetyl chloride or propionyl chloride lead to predominant attack at the nitrogen atom of the heterocycle with production of ring opened products (Equation 16).<sup>10</sup> As an alternative



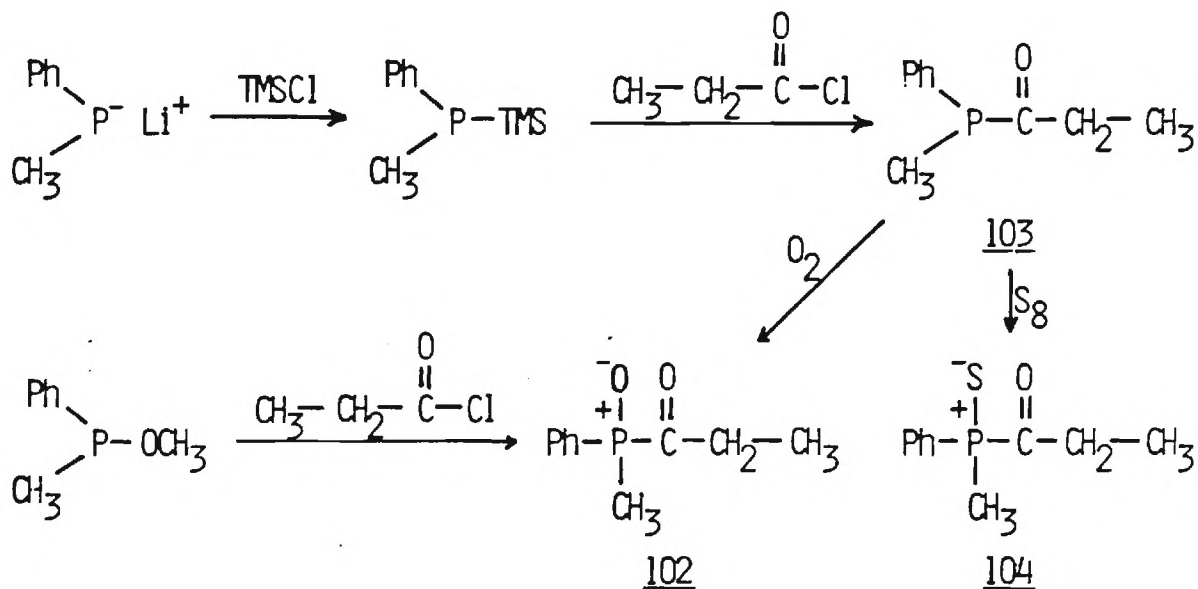
approach **97** was reacted with one equivalent of water in the presence of base to produce **99**. Analysis by  $^1\text{H}$  NMR (300 MHz) revealed that only one diastereomer was formed. Reaction of **99** with potassium *t*-butoxide produced the potassium salt **100**. It was anticipated that, with the formation of the salt, the most nucleophilic atom in the system would now be the phosphorus center. In fact, reaction with methyl iodide produced **101** as one diastereomer. Currently, **100** is being reacted with acid chlorides to form the optically active acyl phosphine oxide directly.



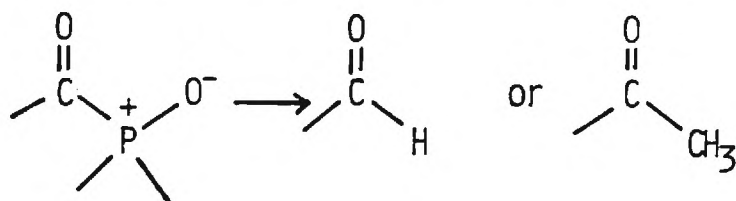
As companion studies to the above, the racemic 120 will be reacted with optically active (R or S)  $\alpha$ -phenylethylalcohol to produce 121. The resulting product will then be separated into its diastereomeric components and each reacted with an acid chloride (under Abrusov conditions) to form an optically active acylphosphine oxide. The asymmetric induction accompanying enolate formation and reaction with benzaldehyde will be determined.



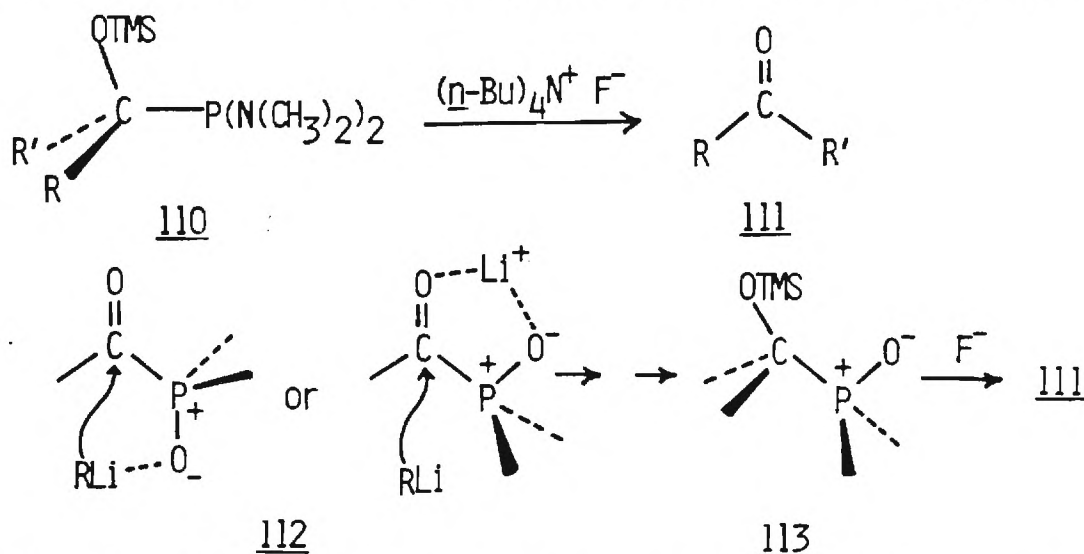
3. In order to explore the simple face selectivity mentioned earlier in this section, racemic propionylphosphine oxide (102), propionylphosphine (103), and propionylphosphine sulfide (104) have been synthesized. Formation of their lithium enolates followed by reaction with benzaldehyde is currently under investigation.



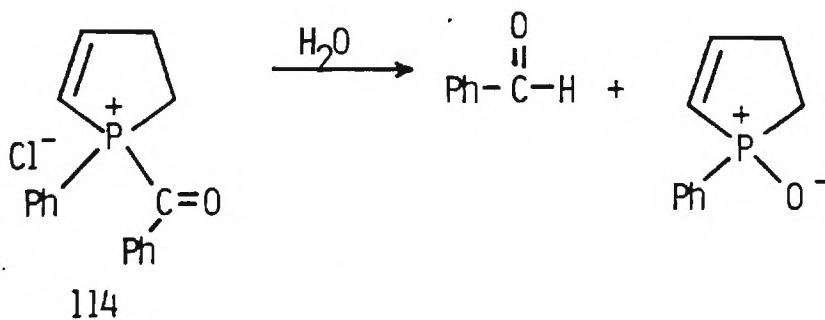
carboxylic acids, amides or esters. Two functional groups of particular interest are carboxaldehyde and ketone functionalities. Evans<sup>83</sup> has reported that



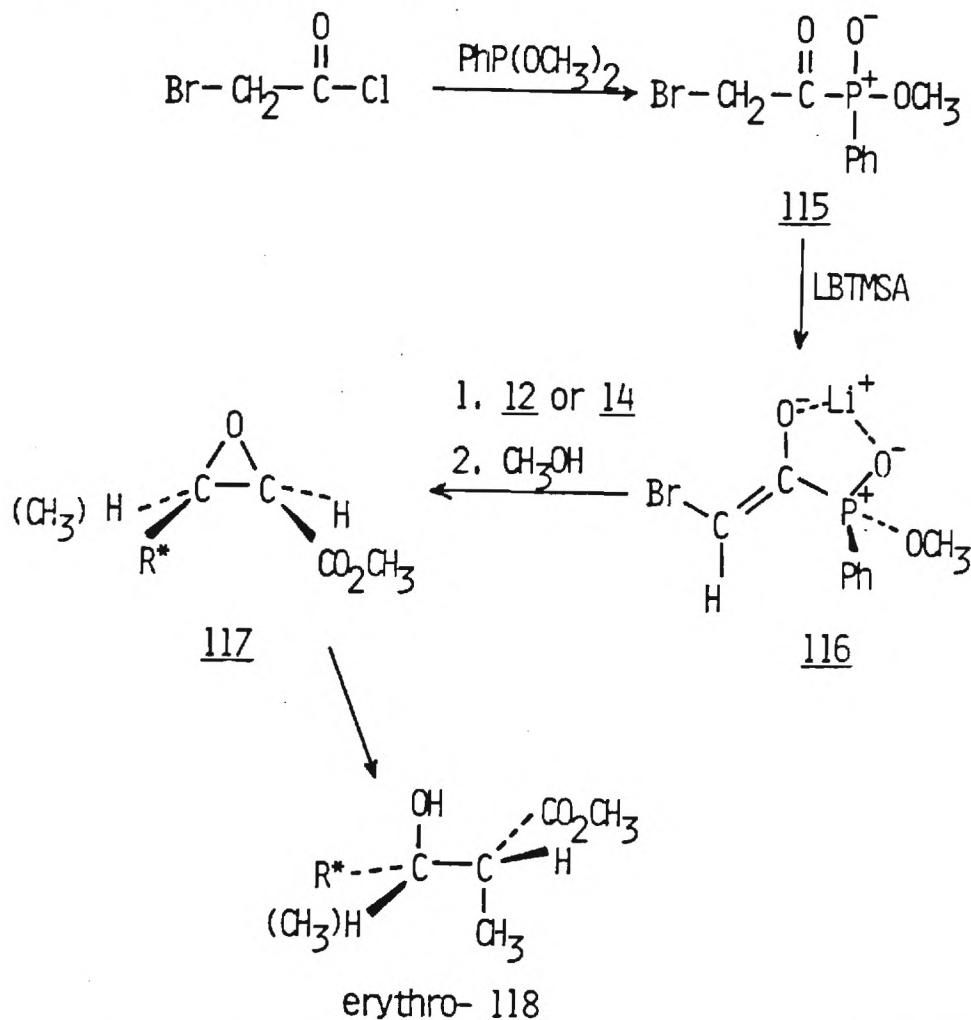
110 undergoes fluorodesilylation to give 111. This suggests that after the utilization of the acylphosphine oxide derivatives in alkylations or aldolizations, the derived products may undergo addition of alkyl lithium reagents followed by silylation to give 113 which, after purification, may be converted into 111. The addition of the organometallic reagent should follow a carbonyl face selective mode via transition state 112 (although this is not particularly important since this center will eventually become achiral).<sup>84</sup> Finally, the



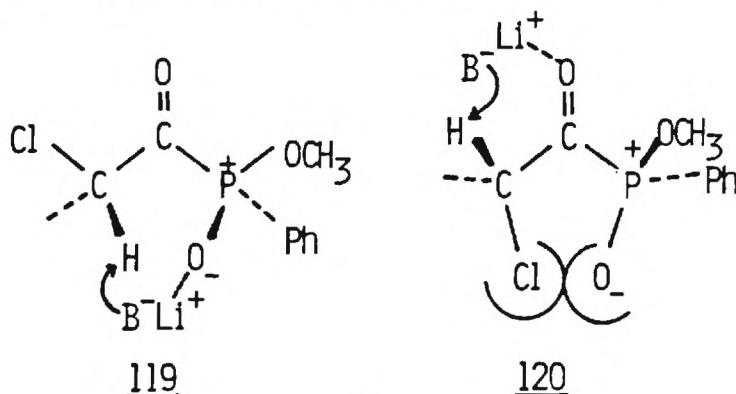
acylphosphonium salt, 114, has been converted to the corresponding aldehyde by hydrolysis. Using analogous technology it is proposed to investigate the following reactions to ultimately provide an aldehyde product from an acylphosphine elaboration.



The Darzens Condensation is of interest in acyclic stereoselection involving asymmetric induction. An  $\alpha$ -bromo enolate should have a low  $E_N$  value relative to an  $\alpha$ -alkyl enolate and thus a smaller approach angle  $\theta$  toward various  $\alpha$ -chiral  $\pi$ -electrophiles. This, of course, should lead to greater asymmetric induction. It is proposed to explore this possibility utilizing the chiral auxilliary substituted enolate 115 in either the stereoselective or enantioselective mode. The following experiments are planned,



The proposed conversion of 115 to the cis-enolate deserves comment. The use of lithium bis-trimethylsilylamide (LBTMSA) to convert  $\alpha$ -bromo ketones to the corresponding enolate is well documented<sup>85</sup>. Such enolates undergo halogen-metal interchange with  $t\text{-BuLi}$  suggesting a cis-relationship between the alkoxide and halogen center<sup>86</sup>. In the case of 115 a large phosphorus substituent would also sterically assist the formation of cis enolate 116 via transition state 119 as opposed to 120. The  $\alpha$ -chiral  $\pi$ -electrophiles 12 and the corresponding methyl ketone 14



will be reacted with cis-enolate 116. It is anticipated that the ketone acceptor will give greater asymmetric induction. From our previous observation concerning the absence of aldolate equilibrium when phosphine oxide auxiliary substituents are employed, one is assured that the initial condensation of 116 with 121 will determine the stereochemistry of the glycidic ester 117. The conversion of 117 to the  $\beta$ -hydroxyester 118 follows from the known stereospecific reaction of glycidic esters with cuprates<sup>87</sup>. In the case of 118 (R=H), comparison to products obtained via aldol routes will be possible.

### Proposed Research-Theoretical

#### Three-Center Trajectory Model-Nucleophilic, Radical and Electrophilic Reactions.

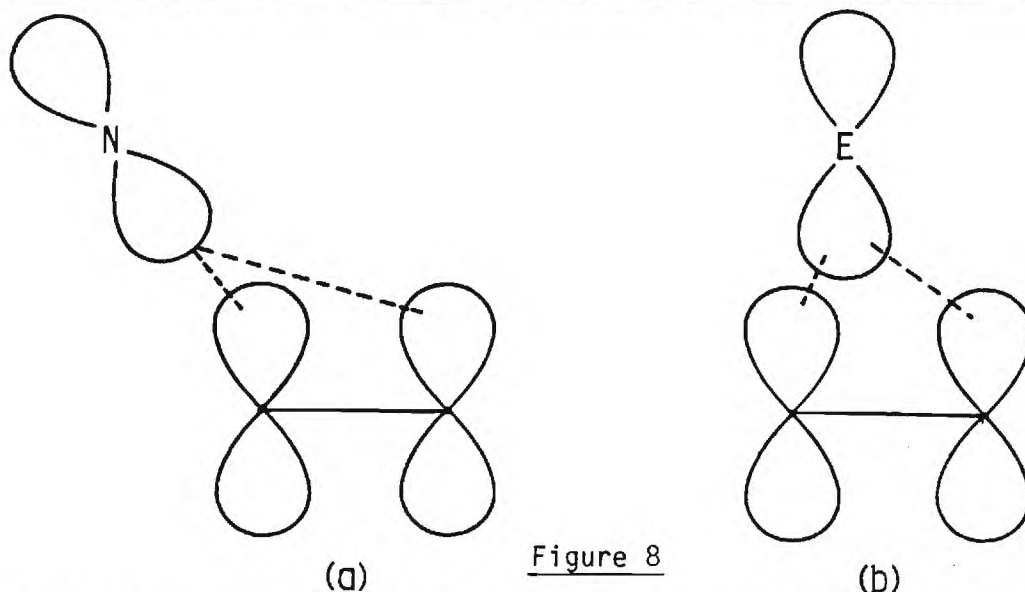


Figure 8

The trajectory model discussed in Appendices A, B, C and D is based upon the interaction of a nucleophilic center (characterized by energy  $E_N$ , atomic orbital coefficient  $c_N$ , and charge  $q_N$ ) with a single center on the  $\pi$ -electrophile. This represents a reasonable approximation since the nucleophile approaches the  $\pi$ -bond at an acute angle (Figure 8a) where because of distance, interaction with one  $\pi$ -center is far greater than interaction with the second  $\pi$ -center. Indeed, valuable generalization concerning asymmetric induction have been elucidated based upon the simple model. In contrast, the approach trajectories of electrophiles is toward the center of the  $\pi$ -bond (Figure 8b) where there is substantial interaction with both  $\pi$ -centers. The trajectories associated with radical species is intermediate between those of nucleophiles and electrophiles. As a consequence, in order to address the asymmetric induction accompanying electrophilic and radical attack at a  $\pi$ -bond possessing an  $\alpha$ -chiral substituent it is proposed to extend the trajectory model to consider more than one  $\pi$ -center. The approach will be similar to that described in Appendix A, B and C in order to preserve simplicity and to easily glean structural generalizations.

#### Electrostatic Mapping: Application to Enzyme-Substrate Specificity

In reviewing the correlation of the theoretical trajectory model with experimental data we were struck by the importance of the electrostatic term. This component of the model was the most important contributor to the differentiation of the stereospecificity of the enolates discussed in Appendix



D. The electrostatic term also was of major importance in the stereochemical differences between the acid and base catalyzed aldol condensations discussed earlier. It is clear that the electrostatic redistribution of electron density and local atomic dipole interactions of a molecule with an approaching charged reagent is an important component of stereochemistry (and regiochemistry) at long ranges ( $>2.0$  angstroms) in early transition state-high charge reactions. However, no systematic correlation of experimental data with any electrostatic model has been made to our knowledge.

The organic chemists has had great success in the prediction of regiochemistry and stereochemistry in the short range region where overlap of atomic orbitals gives rise to charge-transfer and repulsion terms. This type of analysis is, in fact, the basis of the frontier orbital concept of Fukui which was popularized by Houk in analysis of cycloadditions and Woodward-Hoffman in sigmatropic rearrangements. This frontier orbital model was modified by Klopman with incorporation of a simple coulombic term used to differentiate "hard" and "soft" reagents. This modified concept has, likewise, enjoyed considerable success in the analysis of organic and biochemical reactions. We now propose the following questions: Can a simple (and therefore useful) model or set of rules be formulated which will take into account long range electrostatic interactions to complement and/or modify a frontier orbital analysis? Is the model discussed in the Appendix sufficient for this purpose or will it require modification? Is there a simple "frontier" electrostatic model which will correctly predict regiochemistry?

To address these questions a brief review of the concepts and models developed in the past would seem in order. The calculation of intermolecular electrostatic interactions energies has evolved from a multipole expansion for each molecule considered to only a spherical electron density with a net charge (London Model I)<sup>88</sup> to an expansion where the charge density is segmented into regions in the molecule with these regions defined by boundaries at which the charge density changes sign (London Model II). Definition of these boundaries in "overlap space" has been the subject of considerable effort in that they depend upon the selection of the type of function or the atomic orbitals used in the LCAO approach.<sup>90</sup> A simplification, due to Hirschfelder<sup>91</sup>, expands the multipole field about a point defined as the atomic center and having a point charge calculated by a standard SCF method using Slater type atomic orbitals. Finally, a popular method for determining the electrostatic potential at any point to space about a molecule use the density function at the point and coulombs law (Bonaccorsi-Scrocco-Tomasi potentials).<sup>92</sup> This latter method provides only the zeroth order energy in that only ground state wavefunctions are used.

Our model is somewhat different from the above procedures in that no molecular charges at each atomic center are explicitly used. The interaction energy between an atomic center and a charge at long distance is simply the integral of this interaction with the entire electron density approximated by a Slater orbitals scaled by the LCAO coefficients. The multipole expansion is then analytically evaluated for the first-order atomic dipole and second-order atomic dipole charge interaction using a perturbation procedure. In addition, our model was easily extended to the quadrupole moment level. The only input required in the SCF eigenfunctions and eigenvectors and, if these parameters are available from some semiempirical calculation such as MNDO, very large organic and bio-molecules may be analyzed. It should be noted that the existing equations need no modification for analysis of the attack of electrophiles upon nucleophilic molecules.



We have constructed a program (runs on a IBM PC) to determine the electrostatic interaction energy (up to the quadrupole level) at a number of points in a selected plane defined by a target molecule of interest and plot contours of isoenergetic interactions for this system. In this way the channels of approach of a reagents for maximum long range electrostatic stabilization as a function of geometry and atomic centers may be visualized. We hope that a correlation between the observed regio- and stereochemistry of charged molecule reactions and simple SCF parameters such as frontier orbitals, availability of excited states, etc. will be apparent.<sup>93</sup>

This electrostatic mapping procedure is directly applicable to biochemical problems such as enzyme substrate specificity.

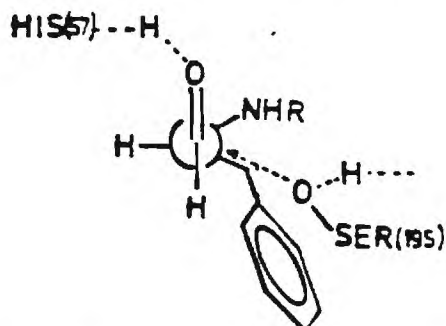
All of the above problems proposed previously were chosen to provide observable tetrahedral products from simple planar prochiral centers. Only in this way could the predictive power of the trajectory model be accessed. However, the conclusions reached with such model studies are immediately applicable to many enzymatic reactions. Consider for example complex substrates which undergo a planar prochiral to chiral tetrahedral and back to planar prochiral reaction sequence at the active site. In such cases the enzyme-bound chiral tetrahedral intermediate is "invisible" to external chemical probes.

Synthetic enzyme inhibitors are designed to mimic the natural substrate with respect to initial binding. The inhibitor may then either remain permanently bound as a tetrahedral intermediate (irreversible binding inhibitors) or then undergo further "unnatural" reactions or rearrangements with the functional groups at the active site (suicide inhibitors). The following proposition is advanced.

Provided binding is the same, efficient synthetic inhibitors are subject to the same trajectory as the natural substrate

To establish the validity of this proposition, we have theoretically examine an enzyme-substrate system, such as the serine proteases primarily because a great deal of experimental information on inhibitors is available.

The active site of a serine protease has been mapped by X-ray crystallography. This protease accepts an aldehyde inhibitor, N-acetylprolylalanylprolylphenylalanyl, whose bound conformation has likewise been mapped to give the following relationship to serine 195:

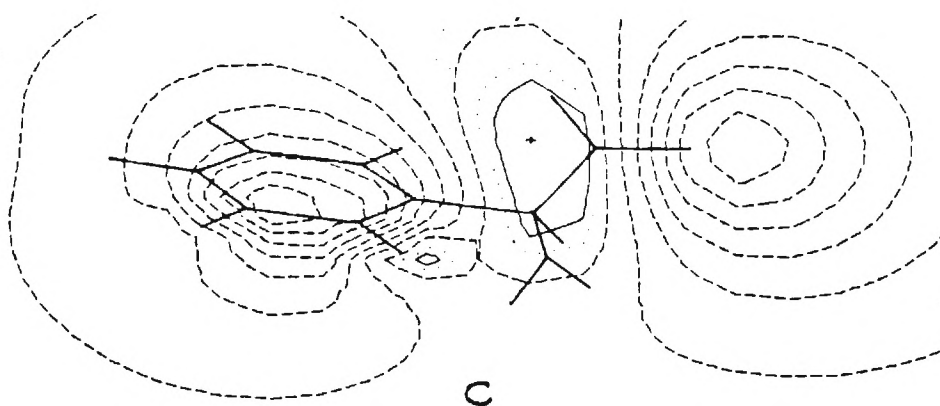
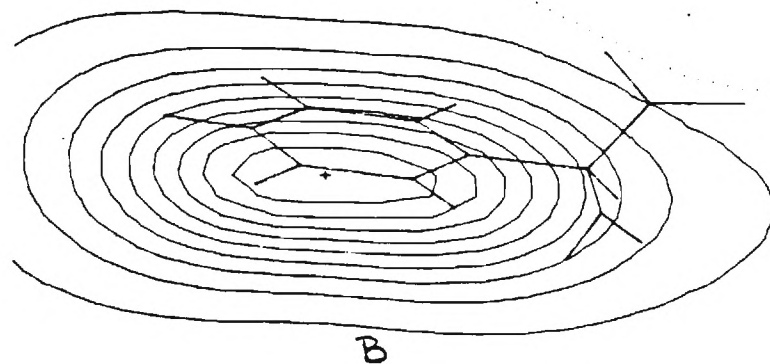
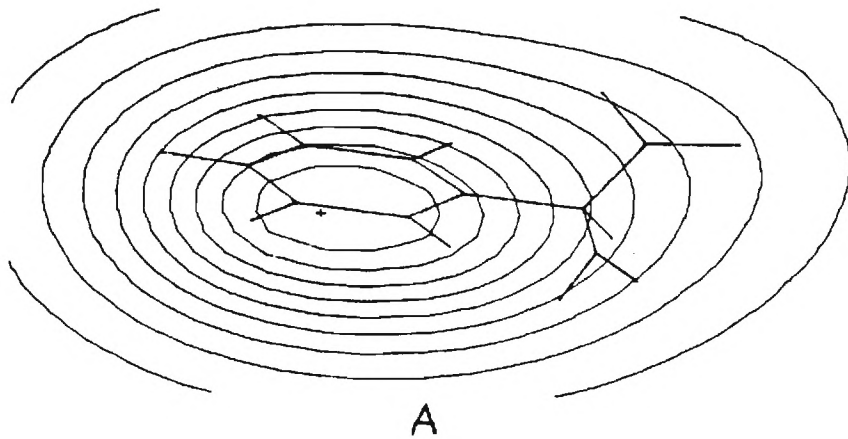
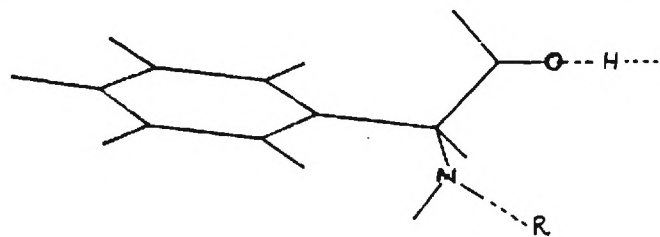


Note that the bound inhibitor is undergoing interaction with serine -195 on the most congested face of the carbonyl group at an angle  $\theta$  which produces an eclipsed steric interaction with a edge-on benzene ring. This is not what would have been predicted by a simple steric mode. This congestion is most evident in an electron density map (A) for the enzyme-substrate complex at 2 Å in a plane parallel to the

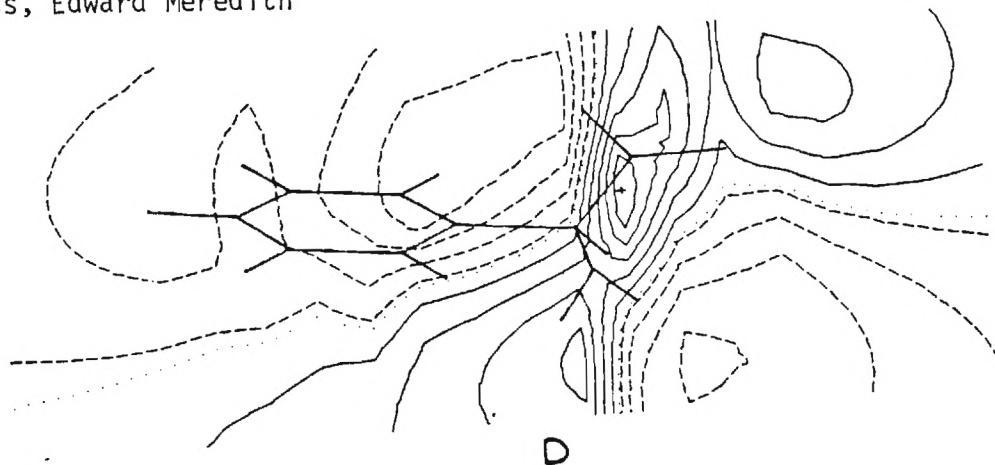
H-C=O groups and in the direction of the serine-195. All density and electrostatic maps shown are in this plane and electrostatic potential contours drawn as solid lines are stabilizing while those as dashed lines are destabilizing. A '+' marks the largest stabilizing potential in the field. The contour values (ev) are shown and the zero contour if any, is drawn as a dotted line. The electrostatic field was mapped with a small (-) test charge representing the attacking serine-195. A charge-transfer map (B) representing the availability of energy-weighted "hole-density" for insertion of the serine-195 electrons arguments for attack at the benzyl system. These two maps (A and B) represent a comprehensive orbital interaction analysis between the bound inhibitor and the serine-195 and indicate that at the orbital level no reaction between the carbonyl group and serine-195 is possible!

However, the electrostatic potential maps provide us with quite a different picture. The monopole map (C) reveals a favorable interaction at just the crystallographic position of the serine-195 oxygen and at almost no other points. The first-order dipole map (D) and second-order dipole map (E) have similar characteristics but in the shift of the favorable potential point toward the carbonyl oxygen. The complex first-order (F) and second-order (E) quadrupole map is dominated by the large quadrupolar field of the benzene ring and nitrogen atom. The quadrupolar interaction of the serine-195 oxygen and nearly edge-on benzene ring is in fact stabilizing and constitutes an interesting anti-steric component to this trajectory!

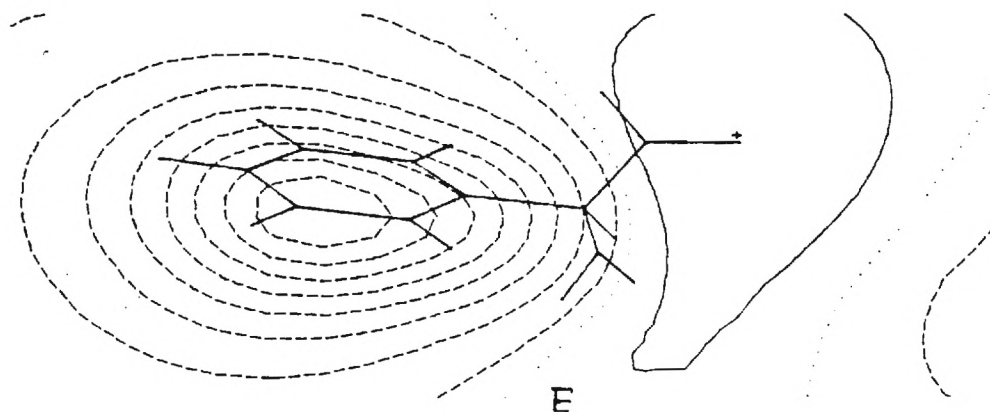
Finally, analysis of this particular enzyme inhibitor problem using classical orbital or steric agreements fails. Our electrostatic analysis provides a new and correct (with regard to experimental facts) approach. Clearly, this model deserves study.



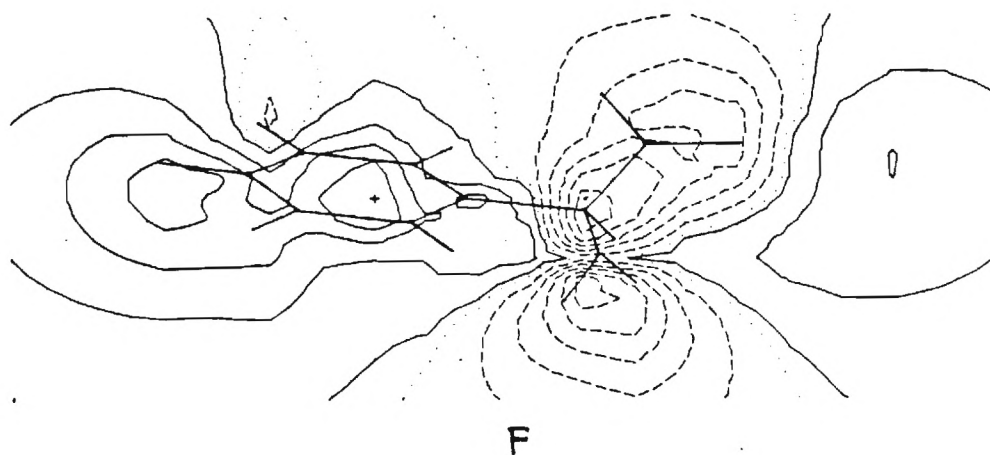
.4873  
-.7640  
-2.0154  
-3.2668  
-4.5182  
-5.7695  
-7.0209  
-8.2723  
-9.5237  
-10.7750



1.7033  
1.3450  
.9867  
.6284  
.2700  
-.0883  
-.4466  
-.8049  
-1.1632  
-1.5215



.0253  
-.0191  
-.0634  
-.1077  
-.1521  
-.1964  
-.2408  
-.2851  
-.3294  
-.3738



3.6718  
2.5543  
1.4367  
.3192  
-.7984  
-1.9159  
-3.0335  
-4.1510  
-5.2685  
-6.3861